DOI: 10.1002/cbic.200900214

Development of Ratiometric Fluorescent Probes for Phosphatases by Using a pK_a Switching Mechanism

Shin Mizukami, Shuji Watanabe, and Kazuya Kikuchi*[a]

The use of fluorescent probes in fluorimetric assays is particularly useful in physiological studies because of their high sensitivity and noninvasiveness. For example, the widely used Ca^{2+} probe fura-2[1] and the subsequently developed fluorescent probes[2] have contributed significantly to the rapid progress of intracellular Ca^{2+} signaling studies. One of the outstanding characteristics of fura-2 is that it exhibits a shift in its excitation spectra in response to changes in Ca^{2+} concentration, which enables ratiometric fluorescence measurement at two wavelengths. Ratiometric measurement, in which the fluorescence intensity is monitored at two excitation or two emission wavelengths and the ratio of the two values is calculated, is more practical than normal fluorescence intensity measurement, because ratiometric measurement can exclude such variables as the influence of dye localization and fluctuation of excitation light intensity.[3]

For the rational design of ratiometric fluorescent probes, the resonance energy transfer (RET) mechanism is quite useful.[4] However, small-molecule RET probes generally require complicated synthesis, which involves conjugation of two different fluorescent dyes. Therefore, a new design principle for ratiometric probes is required. In this study, we developed a novel design strategy for ratiometric fluorescent probes. We applied this strategy in the development of fluorescent probes for detecting phosphatase activity.

Phosphatases catalyze the dephosphorylation of various types of biomolecules, including proteins, nucleic acids, and lipids, and play significant roles in the regulation of metabolic pathways in living organisms. Phosphatases are categorized into several groups, including alkaline phosphatases (ALP),[5] acid phosphatases (ACP),[6] serine/threonine phosphatases,[7] and tyrosine phosphatases (PTP)[8] to name a few. Thus far, several fluorescent probes have been developed for detecting phosphatase activity.[9–12] One prototype is 4-methylumbelliferyl phosphate (MUP),[9] which is hydrolyzed by several types of phosphatases, resulting in an increase in the fluorescence intensity. Other fluorescent phosphatase probes such as 3,6-fluorescein diphosphate (FDP)[10] and 6,8-difluoro-4-methylumbelliferyl phosphate (DiFMUP)[11] are also widely used. However, these probes do not have ratiometric fluorescence properties. Thus, the development of ratiometric fluorimetric probes that can detect phosphatase activities has been attempted by many research groups.

In addition to the aforementioned limitation, known phosphatase probes have another drawback: they have an aryl phosphate monoester moiety; phosphodiesterases convert them to the corresponding aryl alcohol, which fluoresce more strongly than the phosphate monoesters. Although they are considered structural analogues of phosphotyrosine and are used as fluorescent probes for detecting tyrosine phosphatase activity,[11,12] they are hydrolyzed by serine/threonine phosphatases[13] and ALP/ACP.[13,14] Usually, several types of phosphatase are activated in biological samples. When known phosphatase probes such as DiFMUP are used for the detection of phosphatase activity, the output fluorescence signal represents the sum of the activities of several phosphatases. Therefore, there is a requirement for more specific probes for individual phosphatases. For developing a specific probe for a phosphatase, the design of the enzyme-recognizing structure is important. The known probes always require an aryl phosphate monoester structure, and this structural requirement imposes severe limitations on probe design. Herein we report a novel design strategy for fluorescent probes that have an alkyl phosphate monoester structure. We investigated the specificity of the synthesized probes toward several phosphatases and discuss the correlation between their structure and the kinetic parameters in reaction with ACP.

In our design of new ratiometric probes, we initially focused on the fluorescence properties of coumarins. Coumarins containing an electron-donating substituent at the 6- or 7-position generally fluoresce in aqueous solution and have been extensively used for the fluorescence detection of various enzyme activities.[9,11,13,15] In particular, 7-hydroxycoumarins (umbelliferones) have been widely used because they have strong fluorescence intensities and they are easily synthesized. One of their distinctive characteristics is that their fluorescence properties are affected by solution pH;[16] excitation wavelength maxima (λ_{ex}) are approximately 330 and 370 nm in acidic and alkaline solution, respectively (Figure 1 A). This is because the protonation of the 7-hydroxy group affects fluorescence. By varying the pK_a value of the 7-hydroxy group through judicious substitution, the relative proportion of the phenol and phenolate forms in a neutral buffered solution can be systematically varied. Thus, if the pK_a value of the 7-hydroxy group can be controlled by an enzymatic reaction, the excitation spectrum of coumarin would change in response to the enzyme activity.

The conventional approach to vary the pK_a values of 7-hydroxycoumarins involves substitution of the hydrogen atom at the 6- or 8-position with a halogen atom such as fluorine or chlorine; this substitution decreases the pK_a value by an induc-

[a] Dr. S. Mizukami, S. Watanabe, Prof. K. Kikuchi
Division of Advanced Science and Biotechnology
Graduate School of Engineering, Osaka University
2-1 Yamadaoka, Suita, Osaka, 565-0871 (Japan)
Fax: (+81) 6-6879-7924
E-mail: kkikuchi@mls.eng.osaka-u.ac.jp

Supporting information for this article is available on the WWW under http://dx.doi.org/10.1002/cbic.200900214.

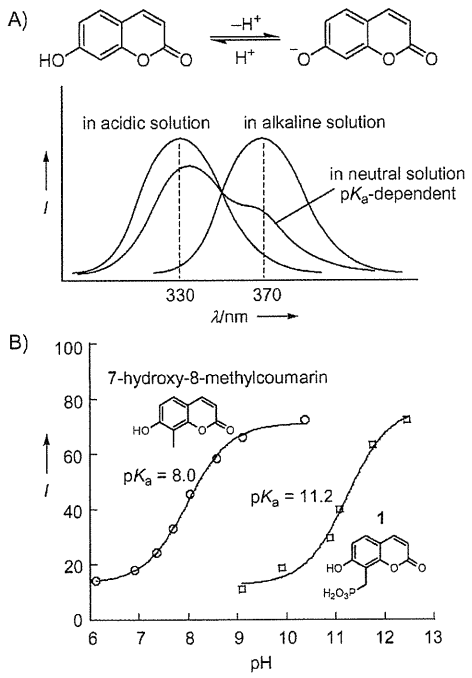

Figure 1. A) pH dependence of the excitation spectra of 7-hydroxycoumarin in aqueous solution (I = fluorescence intensity). B) Effect of a neighboring anionic group on the pK_a values of 7-hydroxycoumarins; fluorescence intensities were measured at λ_{ex} = 380 nm and λ_{em} = 470 nm (25 °C).

tive effect.[17] On the other hand, it has been reported that Calcein Blue (pK_a = 6.9[18]) and other 8-aminomethyl-substituted 7-hydroxycoumarins (pK_a = 6.6–6.7[19]) have lower pK_a values than 7-hydroxy-4-methylcoumarin (pK_a = 7.8[17]). In these cases, the positively charged ammonium groups probably interact with the 7-hydroxy group through hydrogen bonding or electrostatic interactions to enhance deprotonation. By extending this concept, we hypothesized that an anionic group at the 6- or 8-position might increase the pK_a value of the 7-hydroxy group in the opposite manner.

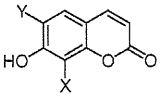

Compound	X	Y
1	$CH_2PO_3H_2$	H
2	$CH_2OPO_3H_2$	H
3a	$CH_2CH_2OPO_3H_2$	H
3b	CH_2CH_2OH	H
4a	H	$CH_2CH_2OPO_3H_2$
4b	H	CH_2CH_2OH
5a	$CH_2CH_2CH_2OPO_3H_2$	H
5b	$CH_2CH_2CH_2OH$	H

To confirm our hypothesis, we synthesized 7-hydroxy-8-phosphorylmethylcoumarin **1** (the synthesis is shown in Scheme S1 in the Supporting Information) and estimated the pK_a value from the fluorescence intensity at various pH values (Figure 1B). As expected, the pK_a value of **1** was considerably higher (pK_a = 11.2) than that of 7-hydroxy-8-methylcoumarin (pK_a = 8.0). This indicates a strong interaction between the anionic phosphate group and the 7-hydroxy group. We exploited this pK_a switch to develop a new type of fluorescent probe, as shown in Figure 2. Here, an anionic group is introduced in the coumarin scaffold at the 6- or 8-position through a tether to increase the pK_a value of the 7-hydroxy group.

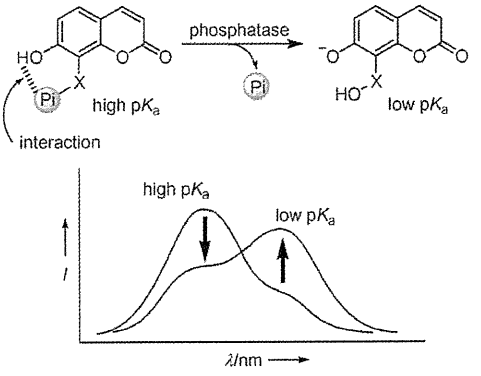

Figure 2. Change in the excitation spectrum of 7-hydroxycoumarin derivatives upon reaction with phosphatases (Pi: phosphate group, X: alkyl linker).

After enzymatic removal of this moiety, the pK_a value would decrease due to loss of the electrostatic interaction, resulting in a change in the excitation spectrum. We selected a phosphate group as the leaving anionic group. In this case, the probe can detect phosphatase activities.

We synthesized 7-hydroxy-8-phosphoryloxymethylcoumarin **2**. However, the compound was unstable and decomposed in aqueous solution. This is probably because the 7-hydroxy group accelerated the removal of the phosphate group to form quinone methide, as reported previously,[16] as phosphate is a good leaving group. We then synthesized **3a**, which has an 8-phosphoryloxyethyl group. We also synthesized **4a** and **5a** in order to examine the effect of the position of the anionic group and the alkyl chain length, respectively. Compounds **3b**–**5b**, lacking phosphate, were synthesized as control compounds. The synthetic routes are shown in Scheme S2 in the Supporting Information.

The pH dependence of the excitation spectrum of **3a** was measured (Figure 3A). Peaks were observed at 333 nm (pH 4.5) and 381 nm (pH 9.3). Between pH 6.5 and 9.3, the excitation spectrum has an isosbestic point at 350 nm; this indicates that only two species, the protonated and deprotonated forms of the 7-hydroxy group, are present in this pH range. The pK_a values of the 7-hydroxy groups of **3a** and **3b** were calculated to be 8.3 and 7.8, respectively, by curve fitting from plots of fluorescence intensity (λ_{ex} = 380 nm, λ_{em} = 470 nm) versus pH (Figure 3B). As we had hypothesized, **3a** showed a greater pK_a value than **3b**.

Compounds **4a** and **5a** showed similar pK_a values (8.1 and 8.2, respectively). The pK_a values of the corresponding dephosphorylated products **4b** and **5b** were 7.7 and 7.8, respectively. In each case, the pK_a value of the phosphate monoester is greater than that of the corresponding alcohol. On the basis of

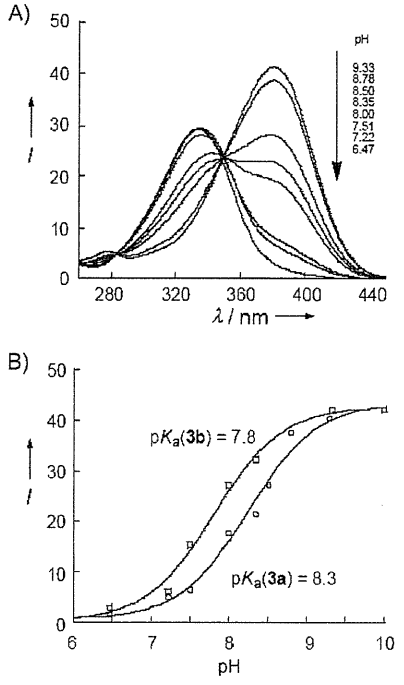

Figure 3. A) Change in the excitation spectrum of **3a** at various pH values (λ_{em}=470 nm). B) Fluorescence intensities of **3a** (○) and **3b** (□) at various pH values (λ_{ex}=380 nm, λ_{em}=470 nm).

these results, it was expected that the excitation spectrum of **3a**–**5a** in neutral buffer solution would change after phosphatase-mediated dephosphorylation, as shown in Figure 2.

We examined the suitability of these compounds as fluorescence probes for phosphatases. When ACP was added to a 10 μM solution of **3a**, the excitation spectrum changed in the expected manner as a function of time. Compounds **4a** and **5a** showed similar spectral changes. For example, the excitation spectrum of **5a** shows a decrease at 330 nm and an increase at 380 nm (Figure 4), originating from the protonated and the deprotonated forms, respectively. The occurrence of the enzyme reaction was confirmed by HPLC (Figure S1, Supporting Information).

Next, we studied the reactivity of other phosphatases toward **3a**. As expected, **3a** was not dephosphorylated by

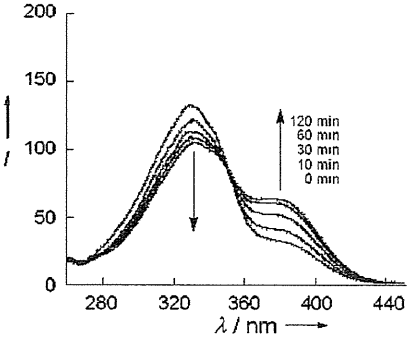

Figure 4. Excitation spectra of **5a** before and after the addition of ACP in 100 mM HEPES buffer solution (pH 7.4) (λ_{em}=470 nm).

PTPs (CD45 and PTP1B) or by serine/threonine phosphatases (PP1 and $PP2A_1$). On the other hand, ALP induced a partial change in the excitation spectrum of **3a**. However, the reaction rate decreased progressively as the reaction proceeded. This result suggests that the reaction product **3b** inhibits ALP activity. To confirm this putative product inhibition, we examined the effect of **3b** on the fluorescence intensity increase of a commercial fluorescent substrate, DiFMUP. The fluorescence intensity of DiFMUP increased significantly after the addition of ALP, whereas pre-incubation with **3b** inhibited this increase (Figure S2, Supporting Information). This supports the view that **3b** causes product inhibition. This inhibition was not observed with the other phosphatases we studied, so this may provide a clue to the development of selective ALP inhibitors. It is also noteworthy that some coumarin derivatives are protein kinase inhibitors.[17]

To examine the properties of the new fluorescent probes more quantitatively, we estimated the parameters K_M and V_{max} of ACP for **3a**–**5a** by fitting the plot of the initial velocity of the enzyme reaction versus substrate concentration with the Michaelis–Menten equation (Table 1). DiFMUP was used as the

Table 1. Kinetic parameters of **3a**, **4a**, and **5a** with acid phosphatase.[a]

Compound	K_M [μM]	$V_{max}\times10^9$ [M min^{-1}]	V_{max}/K_M [min^{-1}]
3a	54±18	4.7±0.3	8.7×10^{-5}
4a	107±27	53±3	5.0×10^{-4}
5a	32±12	17±2	5.3×10^{-4}
DiFMUP	41±19	31±9	7.6×10^{-4}

[a] Kinetic data were measured at 30 °C in 100 mM HEPES buffer (pH 7.4) containing 1.0 mM DTT and 1.0 mM EDTA.

standard substrate under the same conditions. Among the three synthesized probes, **4a** and **5a** showed high V_{max}/K_M values, which were similar to that of DiFMUP, whereas **3a** was the worst substrate. The difference in the V_{max}/K_M values of **3a** and **4a** presumably reflects the difference in steric crowding around the phosphate group, because **3a** and **4a** are regioisomers; that is, **3a** is an 8-substituted coumarin and **4a** is a 6-substituted coumarin, and the 6-position of 7-hydroxycoumarin is less crowded than the 8-position. Compound **5a** had an additional methylene group in the linker, and it showed an approximate sixfold increase in the V_{max}/K_M value in comparison with **3a**. This finding indicates that further modification of the linker group might yield more selective and reactive fluorescent probes for ACP. Our design principle could also be used to develop specific probes not only for ACP but for other phosphatases as well.

In conclusion, we have developed a novel design strategy using a pK_a switching mechanism for the design of ratiometric fluorescent probes to detect phosphatase activity. This design strategy is based on a pK_a shift of the 7-hydroxy group of 7-hydroxycoumarin derivatives induced by an adjacent anionic group, which is directly coupled to a change in the excitation spectrum. The synthesized probes are efficiently dephosphorylated by ACP, and changes in the excitation spectrum are ob-

served. These probes are not dephosphorylated by two protein tyrosine phosphatases (PTP1B and CD45) and serine/threonine phosphatases (PP1 and $PP2A_1$), but are slightly dephosphorylated by ALP. The widely used fluorescent phosphatase probe, DiFMUP, responds to all types of phosphatase activity; therefore, our new probes show different enzyme specificity from previously known probes. The enzyme kinetic data indicate that modification of the linker could dramatically change the enzyme affinity.

Our probe design strategy has afforded ACP-selective fluorescent probes. However, in principle, the probe structure can be changed significantly, provided that the hydroxy group (the 7-hydroxy group in this case) interacts with the ionic group (phosphate group in this case). Thus, this strategy should be applicable to the synthesis of fluorescent probes that are highly specific for various types of phosphatases by modifying the linker structure. Further, as discussed above, ratiometric fluorescent probes are preferable for quantitative bio-imaging experiments. As our probe design strategy intrinsically yields ratiometric probes, it should be helpful for the rational development of a wide range of fluorescent probes for the ratiometric bio-imaging of various hydrolases such as phosphodiesterases and sulfatase in living organisms.

Acknowledgements

This work was supported by MEXT of Japan (Grants 18310144 to K.K. and 19710185 to S.M.), the Special Coordination Funds for the Council of Science and Technology Policy (MEXT and JST), the Mitsubishi Foundation, the Shimadzu Science Foundation, the Kato Memorial Bioscience Foundation, the Astellas Foundation for Research on Metabolic Disorders, the Uehara Memorial Foundation, the Terumo Life Science Foundation, the Nagase Science and Technology Foundation, the Asahi Glass Foundation (to K.K.), and the Cosmetology Research Foundation (to S.M.). S.W. expresses his special thanks for The Global COE Program of Osaka University.

Keywords: coumarin · fluorescent probes · phosphatases · pK_a · ratiometric measurement

[1] G. Grynkiewicz, M. Poenie, R. Y. Tsien, *J. Biol. Chem.* **1985**, *260*, 3440–3450.
[2] a) J. P. Y. Kao, A. T. Harootunian, R. Y. Tsien, *J. Biol. Chem.* **1989**, *264*, 8171–8178; b) H. Iatridou, E. Foukaraki, M. A. Kuhn, E. M. Marcus, R. P. Haugland, H. E. Katerinopoulos, *Cell Calcium* **1994**, *15*, 190–198.
[3] R. Y. Tsien, T. J. Rink, M. Poenie, *Cell Calcium* **1985**, *6*, 145–157.
[4] a) A. Miyawaki, J. Llopis, R. Heim, J. M. McCaffery, J. A. Adams, M. Ikura, R. Y. Tsien, *Nature* **1997**, *388*, 882–887; b) G. Zlokarnik, P. A. Negulescu, T. E. Knapp, L. Mere, N. Burres, L. Feng, M. Whitney, K. Roemer, R. Y. Tsien, *Science* **1998**, *279*, 84–88.
[5] D. W. Moss, *Clin. Chem.* **1982**, *28*, 2007–2016.
[6] D. W. Moss, F. D. Raymond, D. B. Wile, *Crit. Rev. Clin. Lab. Sci.* **1995**, *32*, 431–467.
[7] S. Shenolikar, *Annu. Rev. Cell Biol.* **1994**, *10*, 55–86.
[8] T. R. Burke, Z. Y. Zhang, *Biopolymers* **1998**, *47*, 225–241.
[9] a) H. N. Fernley, P. G. Walker, *Biochem. J.* **1965**, *97*, 95–103; b) D. Robinson, P. Willcox, *Biochim. Biophys. Acta Enzymol.* **1969**, *191*, 183–186; c) J. M. Denu, D. L. Lohse, J. Vijayalakshmi, M. A. Saper, J. E. Dixon, *Proc. Natl. Acad. Sci. USA* **1996**, *93*, 2493–2498.
[10] a) B. Rotman, J. A. Zderic, M. Edelstein, *Proc. Natl. Acad. Sci. USA* **1963**, *50*, 1–6; b) Z. Huang, Q. Wang, H. D. Ly, A. Gorvindarajan, J. Scheigetz, R. Zamboni, S. Desmarais, C. Ramachandran, *J. Biomol. Screening* **1999**, *4*, 327–334.
[11] S. Welte, K.-H. Baringhaus, W. Schmider, G. Müller, S. Petray, N. Tennagels, *Anal. Biochem.* **2005**, *338*, 32–38.
[12] H. Takakusa, K. Kikuchi, Y. Urano, H. Kojima, T. Nagano, *Chem. Eur. J.* **2003**, *9*, 1479–1485.
[13] K. R. Gee, W. C. Sun, R. H. Bhalgat, R. H. Upson, D. H. Klaubert, K. A. Latham, R. P. Haugland, *Anal. Biochem.* **1999**, *273*, 41–48.
[14] Z. Huang, N. A. Olson, W. You, R. P. Hauglamd, *J. Immunol. Methods* **1992**, *149*, 261–266.
[15] a) G. G. Guilbault, J. Hieserman, *Anal. Chem.* **1969**, *41*, 2006–2009; b) J. P. Goddard, J. L. Reymond, *Trends Biotechnol.* **2004**, *22*, 363–370.
[16] D. W. Fink, W. R. Koehler, *Anal. Chem.* **1970**, *42*, 990–993.
[17] W. C. Sun, K. R. Gee, R. P. Haugland, *Bioorg. Med. Chem. Lett.* **1998**, *8*, 3107–3110.
[18] G. M. Huitink, D. P. Poe, H. Diehl, *Talanta* **1974**, *21*, 1221–1229.
[19] M. Adamczyk, M. Cornwell, J. Huff, S. Rege, T. V. S. Rao, *Bioorg. Med. Chem. Lett.* **1997**, *7*, 1985–1988.

Received: April 7, 2009
Published online on May 22, 2009

J|A|C|S COMMUNICATIONS

Published on Web 10/30/2009

Photoactive Yellow Protein-Based Protein Labeling System with Turn-On Fluorescence Intensity

Yuichiro Hori, Hideki Ueno, Shin Mizukami, and Kazuya Kikuchi*

Division of Advanced Science and Biotechnology, Graduate School of Engineering, Osaka University, 2-1 Yamadaoka, Suita, Osaka 565-0871, Japan

Received June 12, 2009; E-mail: kkikuchi@mls.eng.osaka-u.ac.jp

There has been considerable interest in bioimaging technologies for the clarification of protein functions in living systems. So far, fluorescent proteins have made a significant contribution to research on protein expression, localization, and protein−protein interaction.[1] Although various fluorescent proteins (FP) are currently known,[2] it is difficult to visualize proteins in deep tissues, because proteins emitting near-infrared fluorescence, which can pass through thick tissues, are lacking. In addition, the FP size is large (~27 kDa), and therefore, there has been a strong demand for the generation of a smaller protein tag.[3] As an alternative technology, protein labeling systems such as Halo-tag and CLIP-tag have been developed.[4] In these methods, a specific pair of a protein tag and its ligand is employed for detecting proteins of interest. The advantages of these methods are that a variety of fluorescent dyes are potentially available as labeling reagents including near-infrared probes and that the tag proteins are labeled in controlled time. However, in these systems, free probes must be removed by washing cells or purifying cell lysate to distinguish the fluorescence of bound and unbound probes. To solve this issue, our group recently reported on a fluorogenic labeling method.[5] But these tag proteins are still large.[4,5] Although there are some other techniques for protein labeling,[6] they have drawbacks in bioorthogonality or require additional enzyme for protein modification. To overcome these limitations, we utilized photoactive yellow protein (PYP) as a tag protein and developed labeling reagents for this protein, including a fluorogenic probe, which would not require any procedure for removing the free fluorescent probe.

PYP is a small, water-soluble protein found in several purple bacteria.[7] It consists of 125 amino acids (14 kDa) and binds to a natural cofactor, CoA thioester of 4-hydroxycinnamic acid, through transthioesterification with Cys69.[8] In addition to the natural cofactor, it is known that PYP binds to the thioester derivative of 7-hydroxycoumarin-3-carboxylic acid,[9] which is a fluorescent compound. Importantly, PYP and its ligands do not exist in animal cells and, thus, it is expected that PYP expressed in those cells could be bioorthogonally labeled by its exogenous ligand without any cross reaction by endogenous factors. With regard to the design of a fluorogenic labeling system, 7-hydroxycoumarin has an interesting fluorescent property as follows. Previous work shows that a coumarin derivative linked with fluorescein through a flexible linker has no or little fluorescence properties because of the intramolecular association between the dyes and their dissociation triggers the increase in fluorescence intensity.[10] Based on this principle, we designed a probe that consists of 7-hydroxycoumarin-3-carboxylic acid thioester connected to fluorescein through an ethylene glycol linker (Figure 1). It is considered that the probe in the absence of PYP is not fluorescent due to the intramolecular interaction and, once the probe binds to PYP, the coumarin is dissociated from the fluorescein because the interaction between the coumarin and PYP prevents the close contact of two fluorophores.

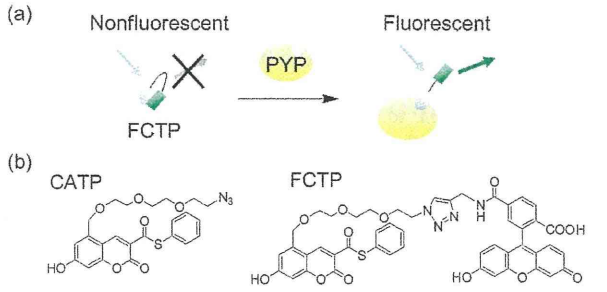

Figure 1. (a) Principle of fluorogenic labeling system based on PYP. (b) Structures of fluorescent probes, CATP and FCTP, for labeling PYP.

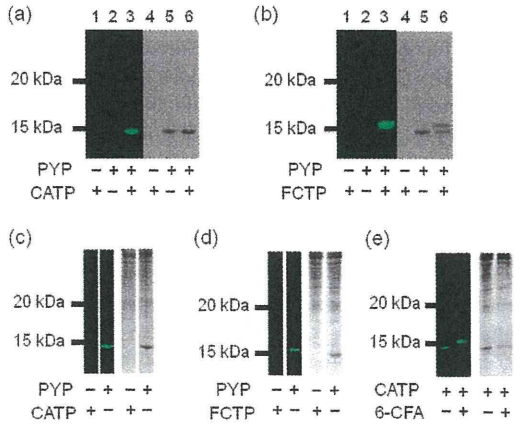

Figure 2. SDS-PAGE analyses of labeling reactions of PYP with probes, CATP and FCTP. Fluorescence and CBB-stained gel images are displayed on the left and right, respectively. PYP (10 μM) was reacted with CATP (25 μM) (a and c) or with FCTP (25 μM) (b and d). Images (c) and (d) represent the reactions in cell lysate. Image (e) represents the stepwise labeling of PYP (5 μM) with CATP (12.5 μM) and 6-CFA (200 μM) in cell lysate.

First, we synthesized CATP, which contains an azido group at the end of the linker (Figure 1b). Considering the steric hindrance, which is predicted from the structure of PYP with its natural cofactor,[11] the linker was introduced into the 5-position in the coumarin, because this position is assumed to be the 2-positon of the natural cofactor based on the structural similarity between these compounds. Then, fluorescein with an alkyne group (6-carboxy-fluorescein propalgylamide, 6-CFA) was conjugated to CATP by click chemistry to generate FCTP (Figure 1b). The probes were incubated with recombinant PYP purified from *E. coli*, and SDS-PAGE analysis was conducted to verify the binding of the probes to the protein (Figure 2a and b). In the absence of the probes, no fluorescence was detected in the gel. In the mixtures of the probes and PYP, fluorescent bands appeared, indicating that the probes bind to PYP. Interestingly, the reaction of FCTP and PYP yielded

10.1021/ja904800k CCC: $40.75

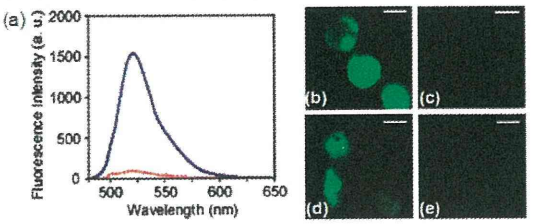

Figure 3. (a) Fluorescence spectra of FCTP (8 μM) in the absence (red dashed line) or presence (blue line) of PYP (5 μM). (b–e) Fluorescent live-cell imaging. Images (b, d) or (c, e) represent the cells that expressed or did not express PYP-PDGFRtm, respectively. The cells after incubation with CATP (5 μM; b, c) or FCTP (20 μM; d, e) are shown. Scale bars = 10 μm.

a slowly migrating band, which is regarded as FCTP-bound PYP because of its fluorescence. The binding of PYP and the probes was also confirmed by MALDI-TOF MS (Figure S1). The addition of CATP or FCTP to PYP gave the mass value of PYP bound to the individual probe, in which thiophenyl ester is replaced by thioester of Cys in the protein. The results indicate that the probes covalently bind to PYP through transthioesterification.

The binding specificity of the probes toward PYP was investigated. Labeling reactions of purified PYP were carried out in the lysate prepared from HEK293T cells. Figure 2c and d show that a single fluorescent band was detected only in the reaction mixture of PYP and each probe, confirming that PYP is specifically labeled by CATP or FCTP under this experimental condition. The influence of free thiols on the labeling reaction was also examined. The presence of a physiological concentration of glutathione (up to 10 mM) did not affect the labeling reactions (Figure S2).[13] Furthermore, the azido moiety of CATP would allow additional labeling of PYP with the second probe by click chemistry and could expand the range of the applications of this system. After the reaction of PYP and CATP in the cell lysate, 6-CFA was added to the reaction mixture in the presence of Cu^{2+} and tris(2-carboxyethyl)phosphine. Electrophoresis revealed a slowly migrating band, as is the case with the FCTP-bound PYP (Figure 2e). There were no newly appearing bands, demonstrating that the stepwise labeling reaction is quite specific.

To examine the fluorogenic properties of FCTP, the fluorescent spectra of the probes were measured (Figure 3a). In the absence of PYP, the fluorescence intensity of FCTP is very weak, suggesting that the coumarin and fluorescein dyes in the probe associate with each other. On the other hand, the binding of PYP and the probe leads to a dramatic increase in the fluorescence intensity. This increase is approximately 20-fold after 24 h of incubation. The result indicates that the coumarin dissociates from the fluorescein due to the formation of the complex between PYP and the probe. We then characterized the binding kinetics of PYP with CATP and FCTP by size exclusion chromatography and fluorescence measurement, respectively (Figures S3 and S4; see Supporting Information for the detailed procedure). The CATP reaction was almost complete within 2 h, consistent with a previous report, demonstrating the binding kinetics of a natural ligand to PYP.[12] In contrast, the binding of FCTP to PYP was slow, requiring more than 24 h to complete the reaction. One probable reason for this difference is that the intramolecular interaction in FCTP could influence its binding kinetics.

Finally, cell labeling experiments were conducted. HEK293T cells expressing PYP-PDGFRtm (the fusion protein of PYP and a transmembrane domain of platelet-derived growth factor receptor) on the cell membrane were prepared. CATP or FCTP was incubated with the cells in culture media. Fluorescence microscopy showed that fluorescent labeling by both probes occurred in the cells expressing PYP-PDGFRtm (Figures 3b and S5). No fluorescence was observed in the cells that did not express PYP-PDGFRtm, demonstrating that PYP is specifically labeled on the cell membrane by both probes. During the experiments, we noticed that CATP was cell-permeable. Therefore, intracellular imaging with CATP was also performed. After the labeling reaction of CATP and the cells expressing maltose binding protein-fused PYP (MBP-PYP) in cytosol, fluorescence was observed only in the cells expressing MBP-PYP, and not in the nonexpressing cells (Figure S5). This result clearly shows that CATP allows specific labeling of PYP inside living cells.

In conclusion, we have developed a protein labeling system, based on a small tag protein, PYP, and its fluorescent probes. The live-cell imaging and specific labeling of PYP were achieved by using CATP and FCTP. CATP has dual functions as a fluorescent probe and a chemical handle for two-step labeling. More importantly, FCTP shows fluorogenic characteristics, allowing the identification of the probe bound to its tag protein. These properties offer a more sophisticated application of this system to protein imaging studies.

Acknowledgment. This work was supported by MEXT of Japan. We thank Prof. Klaas J. Hellingwerf for providing the plasmid encoding PYP and Dr. Aya Fukuda for giving the plasmid for mammalian expression.

Supporting Information Available: Experimental procedures and supplemental results. This material is available free of charge via the Internet at http://pubs.acs.org.

References

(1) (a) Zaccolo, M. *Circ. Res.* **2004**, *94*, 866–873. (b) VanEngelenburg, S. B.; Palmer, A. E. *Curr. Opin. Chem. Biol.* **2008**, *12*, 60–65.
(2) (a) Shaner, N. C.; Steinbach, P. A.; Tsien, R. Y. *Nat. Methods* **2005**, *2*, 905–909. (b) Pakhomov, A. V.; Martynov, V. I. *Chem. Biol.* **2008**, *15*, 755–764.
(3) (a) Zhou, Z.; Koglin, A.; Wang, Y.; McMahon, A. P.; Walsh, C. T. *J. Am. Chem. Soc.* **2008**, *130*, 9925–9930. (b) Chen, I.; Ting, A. Y. *Curr. Opin. Biotechnol.* **2005**, *16*, 35–40.
(4) (a) Los, G. V.; Wood, K. *Methods Mol. Biol.* **2007**, *356*, 195–208. (b) Gautier, A.; Juillerat, A.; Heinis, C.; Corrêa, I. R., Jr.; Kindermann, M.; Beaufils, F.; Johnsson, K. *Chem. Biol.* **2008**, *15*, 128–136.
(5) Mizukami, S.; Watanabe, S.; Hori, Y.; Kikuchi, K. *J. Am. Chem. Soc.* **2009**, *131*, 5016–5017.
(6) (a) O'Hare, H. M.; Johnsson, K.; Gautier, A. *Curr. Opin. Struct. Biol.* **2007**, *17*, 488–494. (b) Wu, P.; Shui, W.; Carlson, B. L.; Hu, N.; Rabuka, D.; Lee, J.; Bertozzi, C. R. *Proc. Natl. Acad. Sci. U.S.A.* **2009**, *106*, 3000–3005. (c) Fernández-Suárez, M.; Baruah, H.; Martínez-Hernández, L.; Xie, K. T.; Baskin, J. M.; Bertozzi, C. R.; Ting, A. Y. *Nat. Biotechnol.* **2007**, *25*, 1483–1487. (d) Nonaka, H.; Tsukiji, S.; Ojida, A.; Hamachi, I. *J. Am. Chem. Soc.* **2007**, *129*, 15777–15779. (e) Adams, S. R.; Campbell, R. E.; Gross, L. A.; Martin, B. R.; Walkup, G. K.; Yao, Y.; Llopis, J.; Tsien, R. Y. *J. Am. Chem. Soc.* **2002**, *124*, 6063–6076.
(7) Kamiuchi, M.; Hara, M. T.; Stalcup, P.; Xie, A.; Hoff, W. D. *Photochem. Photobiol.* **2008**, *84*, 956–969.
(8) Kyndt, J. A.; Meyer, T. E.; Cusanovich, M. A.; Van Beeumen, J. J. *FEBS Lett.* **2002**, *512*, 240–244.
(9) van der Horst, M. A.; Arents, J. C.; Kort, R.; Hellingwerf, K. J. *Photochem. Photobiol. Sci.* **2007**, *6*, 571–579.
(10) Takakusa, H.; Kikuchi, K.; Urano, Y.; Higuchi, T.; Nagano, T. *Anal. Chem.* **2001**, *73*, 939–942.
(11) Anderson, S.; Crosson, S.; Moffat, K. *Acta Crystallogr., Sect. D* **2004**, *60*, 1008–1016.
(12) Imamoto, Y.; Ito, T.; Kataoka, M.; Tokunaga, F. *FEBS Lett.* **1995**, *374*, 157–160.
(13) Wu, G.; Fang, Y. Z.; Yang, S.; Lupton, J. R.; Turner, N. D. *J. Nutr.* **2004**, *34*, 489–492.

JA904800K

J|A|C|S COMMUNICATIONS

Published on Web 03/18/2009

Covalent Protein Labeling Based on Noncatalytic β-Lactamase and a Designed FRET Substrate

Shin Mizukami, Shuji Watanabe, Yuichiro Hori, and Kazuya Kikuchi*

Graduate School of Engineering, Osaka University, 2-1 Yamadaoka, Suita, Osaka 565-0871, Japan

Received October 20, 2008; E-mail: kkikuchi@mls.eng.osaka-u.ac.jp

Fluorescence microscopy is one of the most common techniques employed in the field of life science. With the rapid progress that has been achieved with regard to optical systems, fluorescent proteins (FPs) have acquired important roles for fluorescence microscopy experiments. In order to visualize the localization and behavior of particular proteins of interest, FPs such as green fluorescent protein (GFP) have conventionally been used.[1] More recently, techniques for labeling proteins with small molecules have attracted the attention of many life scientists because they can extend the range of natural FPs, for example, by incorporating near-infrared fluorescent dyes, MRI contrast agents, or biofunctional molecules such as biotin. Several approaches for modifying proteins with small molecules have been commercialized, including methods based on the tetracysteine tag,[2] HaloTag,[3] and SNAP-tag.[4] Other protein labeling methods involving the use of biotin ligase,[5] transglutaminase,[6] hexahistidine,[7] tetra-aspartic acid,[8] etc. have also been reported. Among the abovementioned labeling methods, only the tetracysteine tag exhibits fluorogenic properties. In the other labeling methods, it is necessary to wash the treated cells prior to microscopic measurements to eliminate background fluorescence. Thus, new labeling techniques that satisfy the dual criteria of specificity and fluorogenicity are desirable.

In this paper, we report a specific protein labeling system with an off-on fluorescence switch. It involves covalent modification of a genetically engineered hydrolytic enzyme with a rationally designed fluorogenic probe that exploits the principle of fluorescence resonance energy transfer (FRET). Using this system, we can achieve specific and fluorogenic protein labeling under physiological conditions.

First, we designed the tag protein. Plant or bacterial proteins are preferably used to achieve bioorthogonal labeling in mammalian cells. We focused on β-lactamase as the candidate tag because β-lactamases are small bacterial enzymes that hydrolyze antibiotics containing a β-lactam structure and have no endogenous counterpart among eukaryotic cells.[9] β-Lactamase has been widely used as a reporter enzyme for examining gene expression in living mammalian cells.[10] Class A β-lactamases such as the 29 kDa TEM-1[11] have been extensively investigated with regard to their structures, enzyme reaction kinetics, substrate specificity, inhibitors, etc.[12] The reaction of TEM-1 with β-lactams involves acylation and deacylation steps (Scheme 1). In the acylation step, Ser70 attacks the amide bond of the β-lactam ring to form an intermediate acyl-enzyme complex (ES*). In the deacylation step, an activated water molecule hydrolyzes the ester bond of the intermediate to yield the product. Previous studies have shown that Glu166 is essential for the deacylation step[13] and that the E166N mutant of TEM-1 (^{E166N}TEM) accumulates the acyl-enzyme intermediate by markedly slowing deacylation (k_3) relative to acylation (k_2).[14] We hoped to exploit the properties of the ^{E166N}TEM mutant to covalently attach a fluorescent substrate to β-lactamase.

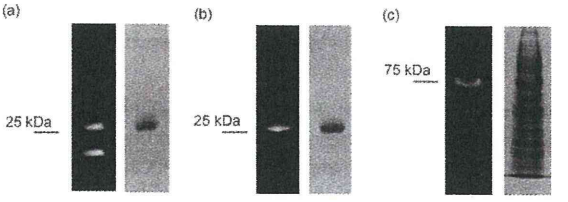

Figure 1. (a, b) Fluorescence (left) and CBB-stained (right) gel images of ^{E166N}TEM after incubation with (a) CA and (b) CCD. (c) Fluorescence and CBB-stained gel image of MBP-^{E166N}TEM mixed with HEK293T cell lysate after incubation with CCD.

Scheme 1. Mechanism of β-Lactam Cleavage by Class A β-Lactamases; (E) Enzyme, (S) Substrate, and (P) Product

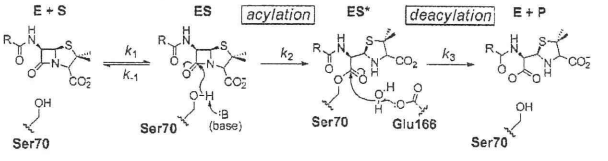

Scheme 2. Structures and Labeling Mechanisms of the Fluorescent Probes (a) CA and (b) CCD

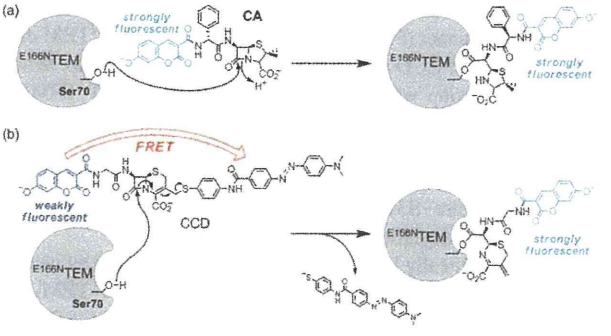

To investigate the feasibility of fluorescently labeling ^{E166N}TEM under physiological conditions, we designed and synthesized a penicillin-based fluorescent probe, coumarinyl ampicillin (CA). The labeling scheme is illustrated in Scheme 2a. Since CA contains 7-hydroxycoumarin, successfully labeled ^{E166N}TEM should exhibit cyan fluorescence. ^{E166N}TEM was incubated with CA in 10 mM Tris-HCl buffer (pH 7.0) at 25 °C, and protein labeling was assessed by SDS-PAGE. Fluorescent proteins were detected by irradiating the gels with UV light at 365 nm. When purified ^{E166N}TEM was mixed with CA, a protein band of ~29 kDa was observed that exhibited cyan fluorescence (Figure 1a); Coomassie Brilliant Blue (CBB) staining confirmed that this band corresponded to ^{E166N}TEM. In contrast, when wild-type (WT) TEM-1 was incubated with CA, no cyan fluorescence was seen (Figure S1a). Although CA successfully labels ^{E166N}TEM, other fluorescent bands were also observed on the gel. Since these bands were also seen when only

10.1021/ja8082285 CCC: $40.75

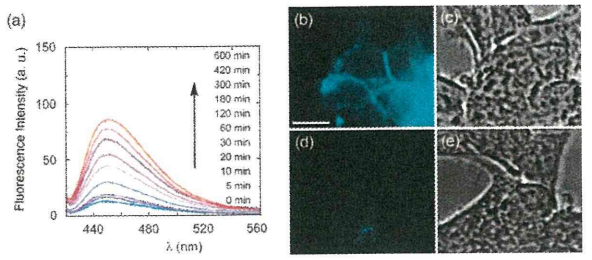

Figure 2. (a) Time-dependent emission spectra (λ_{ex} = 410 nm) of CCD (1 μM) in the presence of ^{E166N}TEM in 100 mM HEPES buffer (pH 7.4) containing 0.1% DMSO at 25 °C. (b–e) Optical microscopic images of CCD-labeled HEK293T cells expressing ^{E166N}TEM-EGFR (b,c) and EGFR (d,e), labeled with 5 μM CCD. (b,d) Fluorescence microscopic images, excitation at 410 nm. (c,e) phase contrast microscopic images. Scale bar: 10 μm.

CA was electrophoresed (Figure S2), a washing procedure should be performed before observation under a fluorescence microscope.

Next, we designed and synthesized CCD (Scheme 2b), a fluorescence off–on labeling probe. This molecule has three main components: 7-hydroxycoumarin, cephalosporin, and 4-(4′-dimethylaminophenylazo)benzoic acid (DABCYL). Since the absorption spectrum of DABCYL substantially overlaps with the emission spectrum of 7-hydroxycoumarin, the fluorescence of CCD would be expected to be largely quenched by intramolecular FRET from coumarin to DABCYL. Based on related probes of β-lactamase activity,[10] cleavage of the β-lactam of CCD by ^{E166N}TEM should result in covalent attachment of the coumarin to the protein with concomitant release of the DABCYL moiety as shown in Scheme 2b. After loss of the DABCYL group, the cyan fluorescence of coumarin should be restored by cancelation of FRET.

The fluorescence spectrum of CCD confirmed that the coumarin fluorescence was almost completely quenched because of FRET. The fluorescence quantum yield of CCD was 0.006, which is much lower than that of CA (Φ = 0.40). When CCD was incubated with ^{E166N}TEM, the fluorescence increased considerably in a time-dependent manner (Figure 2a). This indicates that ^{E166N}TEM cleaved the β-lactam of CCD and eliminated the DABCYL group. When the DABCYL group was completely eliminated by WT TEM-1, the fluorescence signal increased approximately 30-fold. The apparent rate of reaction between CCD and ^{E166N}TEM was approximately 80-fold slower than that of the reaction between CCD and WT TEM-1 (Figure S3), probably because the mutation at E166 decreases the acylation rate (k_2) somewhat.[15]

CCD specifically labels ^{E166N}TEM, as demonstrated by incubation of the probe molecule with both ^{E166N}TEM and WT TEM-1 in 10 mM Tris-HCl buffer (pH 7.0) at 25 °C, followed by SDS-PAGE analysis. As shown in Figure 1b, only the band corresponding to ^{E166N}TEM exhibited cyan fluorescence; no fluorescence was associated with WT TEM-1 (Figure S1b). In contrast to CA, unreacted CCD yielded considerably weaker fluorescence on the gel. In MALDI-TOF MS analyses of the samples, the molecular mass peak for the protein–probe adduct was only detected when ^{E166N}TEM was incubated with CCD (Figure S4).

This system can therefore be used to label target proteins in a biological medium. For example, we fused ^{E166N}TEM to maltose binding protein (MBP, 42 kDa), mixed the purified MBP–^{E166N}TEM construct with HEK293T cell lysate, and incubated the mixture with CCD at 25 °C for 45 min. SDS-PAGE analysis revealed that fusion protein was efficiently and selectively labeled with the fluorogenic probe (Figure 1c).

Finally, we investigated specific labeling of target proteins displayed on the surface of living cells. ^{E166N}TEM was fused to the N-terminus of epidermal growth factor receptor (EGFR), a membrane associated protein, and the construct was produced in HEK293T cells. After treatment with CCD (see Supporting Information), the cells were examined under a fluorescence microscope. Only cells producing the ^{E166N}TEM-EGFR fusion protein emitted cyan fluorescence as a consequence of specific labeling by the probe (Figure 2b–e).

In conclusion, we have developed a novel protein labeling system that combines a genetically modified β-lactamase with low molecular weight fluorogenic β-lactam probes. Through appropriate probe design, we succeeded in labeling proteins with a sensitive fluorophore in vitro and on living cells. In principle, this system does not require washing procedures to remove the unreacted probes after labeling. Furthermore, since the ^{E166N}TEM tag protein is absent in mammalian cells, it can be used for the specific labeling of proteins in higher eukaryotes. We anticipate that this labeling system will find wide application in the field of life science.

Acknowledgment. We thank Dr. Shahriar Mobashery at the University of Notre Dame for kindly providing TEM-1 plasmid. We also thank Dr. Robert E. Campbell at Alberta University, Dr. Gregor Zlokarnik at Vertex Pharmaceuticals, and Dr. Donald Hivert at ETH Zürich for helpful discussions. S.W. acknowledges a Global COE Fellowship of Osaka University. This work was supported in part by MEXT of Japan.

Supporting Information Available: Detailed experimental procedures and supplementary figures. This material is available free of charge via the Internet at http://pubs.acs.org.

References

(1) Chudakov, D. M.; Lukyanov, S.; Lukyanov, K. A. *Trends Biotechnol.* **2005**, *23*, 605–613.
(2) Griffin, B. A.; Adams, S. R.; Tsien, R. Y. *Science* **1998**, *281*, 269–272.
(3) Los, G. V.; et al. *ACS Chem. Biol.* **2008**, *3*, 373–382.
(4) Keppler, A.; Gendreizig, S.; Pick, H.; Vogel, H.; Johnsson, K. *Nat. Biotechnol.* **2003**, *21*, 86–89.
(5) Chen, I.; Howarth, M.; Lin, W.; Ting, A. Y. *Nat. Methods* **2005**, *2*, 99–104.
(6) Lin, C.-W.; Ting, A. Y. *J. Am. Chem. Soc.* **2006**, *128*, 4542–4543.
(7) Hauser, C. T.; Tsien, R. Y. *Proc. Natl. Acad. Sci. U.S.A.* **2007**, *104*, 3693–3697.
(8) Ojida, A.; Honda, K.; Shinmi, D.; Kiyonaka, S.; Mori, Y.; Hamachi, I. *J. Am. Chem. Soc.* **2006**, *128*, 10452–10459.
(9) Waley, S. G. *In the chemistry of β-lactams*; Page, M. I., Ed.; Chapman & Hall: London, 1992; p 198.
(10) (a) Moore, J. T.; Davis, S. T.; Dev, I. K. *Anal. Biochem.* **1997**, *247*, 203–209. (b) Zlokarnik, G.; Negulescu, P. A.; Knapp, T. E.; Mere, L.; Burres, N.; Feng, L.; Whitney, M.; Roemer, K.; Tsien, R. Y. *Science* **1998**, *279*, 84–88. (c) Gao, W.; Xing, B.; Tsien, R. Y.; Rao, J. *J. Am. Chem. Soc.* **2003**, *125*, 11146–11147. (d) Campbell, R. E. *Trends Biotechnol.* **2004**, *22*, 208–211. (e) Xing, B.; Khanamiryan, A.; Rao, J. *J. Am. Chem. Soc.* **2005**, *127*, 4158–4159.
(11) Sutcliffe, J. G. *Proc. Natl. Acad. Sci. U.S.A.* **1978**, *75*, 3737–3741.
(12) Matagne, A.; Lamotte-Blasseur, J.; Frére, J.-M. *Biochem. J.* **1998**, *330*, 581–598.
(13) Guillaume, G.; Vanhove, M.; Lamotte-Brasseur, J.; Ledent, P.; Jamin, M.; Joris, B.; Frére, J.-M. *J. Biol. Chem.* **1997**, *272*, 5438–5444.
(14) Adachi, H.; Ohta, T.; Matsuzawa, H. *J. Biol. Chem.* **1991**, *266*, 3186–3191.
(15) Vijayakumar, S.; Ravishanker, G.; Pratt, R. F.; Beveridge, D. L. *J. Am. Chem. Soc.* **1995**, *117*, 1722–1730.

JA8082285

J|A|C|S COMMUNICATIONS

Published on Web 06/29/2010

Photocontrolled Compound Release System Using Caged Antimicrobial Peptide

Shin Mizukami,[†,‡] Mariko Hosoda,[†] Takafumi Satake,[†] Satoshi Okada,[†] Yuichiro Hori,[†] Toshiaki Furuta,[§] and Kazuya Kikuchi*[,†,‡]

Division of Advanced Science and Biotechnology, Graduate School of Engineering, and Immunology Frontier Research Center, Osaka University, Osaka 565-0871, Japan, and Department of Biomolecular Science and Research Center for Materials with Integrated Properties, Toho University, Chiba 274-8510, Japan

Received March 15, 2010; E-mail: kkikuchi@mls.eng.osaka-u.ac.jp

Abstract: A novel photocontrolled compound release system using liposomes and a caged antimicrobial peptide was developed. The caged antimicrobial peptide was activated by UV irradiation, resulting in the formation of pores on the liposome surface to release the contained fluorophores. The compound release could be observed using fluorescence measurements and time-lapse fluorescence microscopy. UV irradiation resulted in a quick release of the inclusion compounds (within 1 min in most cases) under simulated physiological conditions. The proposed system is expected to be applicable in a wide range of fields from cell biology to clinical sciences.

Caged compounds are photoactivatable probes that are biologically or functionally inert prior to their uncaging. Photoactivation of a caged compound enables the spatiotemporal regulation of various biomolecules of interest in living cells or tissues. Thus, photoactivation technologies using caged compounds have been used as powerful tools in recent biological studies. Various caged compounds such as Ca^{2+}, neurotransmitters, nucleotides, peptides, and enzymes have been reported thus far.[1] Caged compounds provide biologists with valuable tools for investigating biological phenomena. However, current caging/uncaging systems require the synthesis of individual caged compounds for each target biomolecule. Because such syntheses generally entail complicated and multistep reactions, the development of a new methodology is desired for enabling the widespread use of photoactivation technology that can be applicable to various biomolecules ranging from small molecules to macromolecules such as proteins and nucleic acids.

We presume that a nano- or microscale photodegradable "cage" can be used for this purpose. This photoactivation system is essentially similar to the controlled drug release systems investigated from a clinical perspective.[2] Among the various drug carriers, liposomes have been actively developed;[3] further, various types of photoinduced drug-releasing liposomes have been reported. Such functional liposomes generally consisted of designed lipids such as photoisomeric lipids[4] or photocaged lipids.[5] Very recently, photoinduced drug release systems using photocaged dendrons[6] or polymeric microcapsules functionalized with bacteriorhodopsin[7] have also been reported. Nevertheless, the development of a new and practical photocontrolled release system is still strongly required. In this paper, we report a novel photocontrolled release system that works on the basis of a strategy that is clearly different from previously known strategies.

In our proposed system, a photoresponsive drug carrier was divided into two parts: a drug carrier and a photoresponsive opener.

Chart 1. Structures of TL and BTL

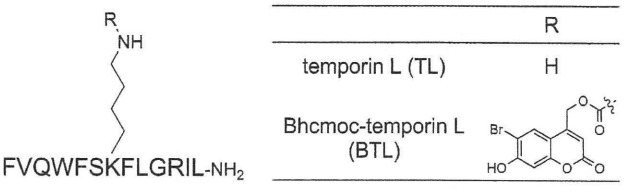

We selected liposomes as the drug carriers because of their versatility and biocompatibility. While selecting the photoresponsive opener, we focused on the membrane-damaging properties of antimicrobial peptides (AMPs).[8] AMPs have attracted increasing attention as a new category of antibiotics. In natural systems, AMPs target the lipid bilayers of bacterial membranes and kill the bacteria by disrupting their membranes. AMPs also degrade liposomes whose compositions are similar to those of the bacterial membrane. Therefore, we assumed that this membrane-damaging property can be applied to construct a photocontrolled drug release system.

We designed a protected AMP derivative Bhcmoc-temporin L (BTL) (Chart 1). BTL consists of a short antimicrobial peptide temporin L (TL),[8b,c] which was isolated from the European red frog *Rana temporaria*, and a photoremovable 6-bromo-7-hydroxycoumarin-4-ylmethyloxycarbonyl (Bhcmoc) group.[9] The Bhcmoc group was attached to the ε-amino group of the Lys. The positively charged amino acid residues of AMPs play important roles in the bacterial membrane damaging properties of AMPs.[8] Thus, protective modification of the Lys in TL was expected to reduce its membrane damaging properties. It was assumed that after the protective group was removed using UV irradiation, its membrane damaging properties would be recovered. As shown in Figure 1, we expected that the combination of BTL and a liposome having the same lipid composition as the bacterial outer membranes would provide a UV-responsive drug release system.

BTL was synthesized in the following two steps: solid-phase Fmoc peptide synthesis and subsequent modification of the Bhcmoc group (Scheme S1 in the Supporting Information). All the synthetic procedures were performed on resins, and the final product was

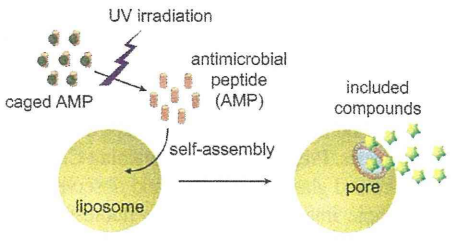

Figure 1. Schematic diagram of photocontrolled release system using caged antimicrobial peptide.

[†] Division of Advanced Science and Biotechnology, Graduate School of Engineering, Osaka University.
[‡] Immunology Frontier Research Center, Osaka University.
[§] Toho University.

10.1021/ja102167m

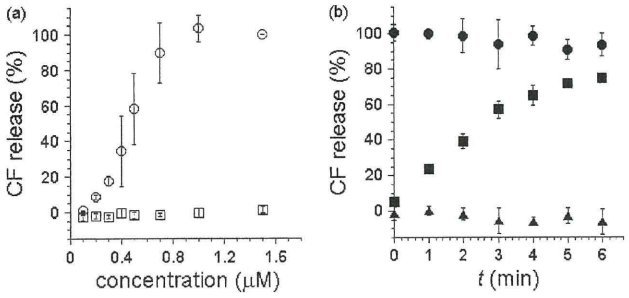

Figure 2. CF release from LUVs induced by synthesized compounds. Lipid concentration: 2.5 μg/mL. Error bars indicate the SD ($n = 3$). (a) Correlation between CF release and concentration of compounds (circles: TL, squares: BTL) under dark conditions. (b) Correlation between CF release and UV irradiation time t in the presence of 4 μM compounds (circles: TL, squares: BTL, triangles: none).

purified by reversed-phase HPLC after the cleavage from the resin and was identified by ESI-TOF MS.

The UV-light-induced conversion of BTL to TL was confirmed using HPLC analysis. Over 95% of BTL underwent conversion within 5 min of UV irradiation; simultaneously a few new peaks emerged in the HPLC analysis (Figure S1 in the Supporting Information). One of these new peaks was assigned to TL. Thus, it was confirmed that BTL was converted to TL using UV light.

Next, we examined whether or not the membrane-damaging property of TL was nullified by the modification of the Lys residue with the Bhcmoc group. Liposomes containing fluorescence dyes have been utilized as a standard tool for the evaluation of the membrane-damaging activities of AMPs and their mimics.[10] When the AMPs disrupt the lipid membrane of the liposomes, the dyes in the liposomes are released. We prepared large unilamellar vesicles (LUVs) and 5(6)-carboxyfluorescein (CF) as the encapsulated fluorescence dye. Since the fluorescence of CF in LUVs is partly quenched because of the high concentration effect, the collapse of the LUV membrane induces the increase in the fluorescence. A fraction of the release activity was estimated using this increase in the fluorescence. As shown in Figure 2a, addition of TL induced the release of CF with a concentration in the submicromolar range. In contrast, BTL did not induce the leakage of CF with a several micromolar concentration. These results indicate that the modification of the Bhcmoc group at the Lys of TL drastically reduced its membrane damaging property. In addition, CD spectra of TL and BTL showed that substitution at the Lys negatively affects the α-helix formation in the presence of liposomes (Figure S2 in the Supporting Information).

Next, the photocontrolled release of CF from LUVs was examined by using BTL and applying UV irradiation. LUV solutions were irradiated using a UV lamp for various periods of time in the presence or absence of BTL. The lamp was then switched off for 60 s, after which the fluorescence intensities of the sample were measured. In the presence of BTL, a fraction of the CF release was dependent on the UV exposure time (Figure 2b). UV irradiation in the absence of BTL did not induce CF release. Thus, photocontrolled release was achieved by the appropriate adjustment of the BTL concentration and UV exposure time.

Finally, the applicability of the photocontrolled release system to fluorescence microscopic studies was examined. Giant unilamellar vesicles (GUVs) were selected for this purpose, because GUVs have larger diameters and the changes in their shape can be observed using optical microscopes. Prepared GUVs containing CF were loaded on a poly-L-lysine-coated glass-bottom dish and observed using a fluorescence microscopic imaging system. The fluorescence images were captured by the excitation of visible light ($\lambda = 460-490$ nm). The

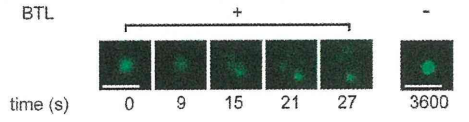

Figure 3. Fluorescence microscopic images of GUVs containing CF under UV irradiation in the presence (12.5 μM) or absence of BTL. Scale bar: 10 μm.

GUVs were stable for several hours under the experimental conditions. When 12.5 μM TL was added, the fluorescence of the GUVs completely disappeared within 40 s, although the addition of 12.5 μM BTL did not induce the disruption of GUVs (data not shown). The GUVs were then irradiated by UV light ($\lambda = 330-385$ nm) using a fluorescence microscope. In the absence of BTL, the GUVs were stable under the microscopic UV excitation. On the other hand, in the presence of BTL, leakage of the CF from the GUVs mostly with the membrane blebbing was observed within tens of seconds under the UV irradiation (Figure 3). In most cases, the leakage was completed within 1 min.

In conclusion, we developed a novel photocontrolled release system by combining liposomes and a caged antimicrobial peptide. This system was experimentally found to be effective for liposomes of different sizes. The response to UV irradiation was rapid, and the release was induced under simulated physiological conditions and also under the experimental conditions of time-lapse fluorescence microscopy. These data imply that this system could be applicable to fluorescence imaging for living cells or living animals. Because liposomes tolerate a wide variety of inclusion compounds from small molecules to macromolecules, this system could enable the development of a universal photouncaging system that might offer a breakthrough in biological studies. Further, in terms of clinical applications, this technology might be applied to other external stimuli such as specific enzyme activities in diseased tissues. This controlled release system may be useful in a wide range of research fields from cell biology to clinical medicine.

Acknowledgment. We thank Drs. Shigenori Kanaya and Yuichi Koga at Osaka University for the use of CD spectrometer. This work was supported in part by MEXT of Japan. S.M. thanks the Cosmetology Research Foundation.

Supporting Information Available: Detailed experimental procedures and supplementary results. This material is available free of charge via the Internet at http://pubs.acs.org.

References

(1) Mayer, G.; Heckel, A. *Angew. Chem., Int. Ed.* **2006**, *45*, 4900–4921.
(2) (a) Rapoport, N. *Prog. Polym. Sci.* **2007**, *32*, 962–990. (b) Shum, P.; Kim, J.-M.; Thompson, D. H. *Adv. Drug Delivery Rev.* **2001**, *53*, 273–284. (c) Chilkoti, A.; Dreher, M. R.; Meyer, D. E.; Raucher, D. *Adv. Drug Delivery Rev.* **2002**, *54*, 613–630. (d) Schmaljohann, D. *Adv. Drug Delivery Rev.* **2008**, *58*, 1655–1670.
(3) Torchilin, V. P. *Nat. Rev. Drug Discov.* **2005**, *4*, 145–160.
(4) (a) Bisby, R. H.; Mead, C.; Morgan, C. G. *Biochem. Biophys. Res. Commun.* **2000**, *276*, 169–173. (b) Liu, X.-M.; Yang, B.; Wang, Y. L.; Wang, J.-Y. *Chem. Mater.* **2005**, *17*, 2792–2795.
(5) (a) Zhang, Z.-Y.; Smith, B. D. *Bioconjugate Chem.* **1999**, *10*, 1150–1152. (b) Watanabe, S.; Hiratsuka, R.; Kasai, Y.; Munakata, K.; Takahashi, Y.; Iwamura, M. *Tetrahedron* **2002**, *58*, 1685–1691. (c) Chandra, B.; Subramaniam, R.; Mallik, S.; Srivastava, D. K. *Org. Biomol. Chem* **2006**, *4*, 1730–1740.
(6) Park, C.; Lim, J.; Yun, M.; Kim, C. *Angew. Chem., Int. Ed.* **2008**, *47*, 2959–2963.
(7) Erokhina, S.; Benassi, L.; Bianchini, P.; Diaspro, A.; Erokhin, V.; Fontana, M. P. *J. Am. Chem. Soc.* **2009**, *131*, 9800–9804.
(8) (a) Zasloff, M. *Nature* **2002**, *415*, 389–395. (b) Mahalka, A. K.; Kinnunen, P. K. J. *Biochim. Biophys. Acta* **2009**, *1788*, 1600–1609. (c) Rinaldi, A. C.; Mangoni, M. L.; Rufo, A.; Luzi, C.; Barra, D.; Zhao, H.; Kinnunen, P. K. J.; Bozzi, A.; Giulio, A. D.; Simmaco, M. *Biochem. J.* **2002**, *368*, 91–100.
(9) (a) Furuta, T.; Wang, S. S.; Dantzker, J. L.; Dore, T. M.; Bybee, W. J.; Callaway, E. M.; Denk, W.; Tsien, R. Y. *Proc. Natl. Acad. Sci. U.S.A.* **1999**, *96*, 1193–1200. (b) Ando, H.; Furuta, T.; Tsien, R. Y.; Okamoto, H. *Nat. Genet.* **2001**, *28*, 317–325. (c) Furuta, T.; Watanabe, T.; Tanabe, S.; Sakyo, J.; Matsuda, C. *Org. Lett.* **2007**, *9*, 4717–4720.
(10) Tew, G. N.; Liu, D.; Chen, B.; Doerksen, R. J.; Kaplan, J.; Carroll, P. J.; Klein, M. L.; DeGrado, W. F. *Proc. Natl. Acad. Sci. U.S.A.* **2002**, *99*, 5110–5114.

JA102167M

Turn-on fluorescence switch involving aggregation and elimination processes for β-lactamase-tag†

Kalyan K. Sadhu,[a] Shin Mizukami,[ab] Shuji Watanabe[a] and Kazuya Kikuchi*[ab]

Received 8th July 2010, Accepted 13th August 2010
DOI: 10.1039/c0cc02432e

The targeted protein of interest is fused with genetically modified β-lactamase enzyme, which reacts with the probe in physiological conditions to break the aggregated interaction between the fluorophore and quencher. This alliance–separation technique is new for protein labeling and is probed *in vitro* and in live cell imaging studies.

Molecular imaging with the aid of fluorescence microscopy has become an indispensable means to study the proceedings in living cells, which would be extensively valuable for the future of medical science. The practical approach involving chemistry to control modification and monitoring specific proteins has proved useful.[1] The direct imaging of protein interactions in single living cells is possible due to the site-specific labeling of proteins with molecular tags, which is an authoritative means for studying the structure–function relationships of proteins.[2] The rationale of fluorescence microscopy in cell biology has been thoroughly tailored with fluorescence proteins.[3] To conquer the shortcomings intrinsic to proteins due to the lack of robust modification for target phenomena and nonfluorogenicity, bright and photostable small fluorophores can be advantageous over their fluorescent protein counterparts.[4] Tetracysteine-tag and its modified version provided a route for using small molecules in fluorogenic labeling and were found to be effective for activation of G protein-coupled receptors in living cells.[5] Specificity towards labeling was observed with SNAP-tag and its modified version with semisynthetic fluorescent sensor proteins.[6] In our protein labeling method our aim was to combine fluorogenicity and specificity of the probe. Several other protein-[7] and enzyme-mediated[8] labeling methods have enriched the recent literature. Among the small fluorogenic molecules, fluorescein is approved by the U.S. Food and Drug Administration (FDA) for medical use.[9] Herein, we have chosen fluorescein for our protein labeling experiment.

Recently we have shown[10] a protein labeling system that coalesces genetically modified β-lactamase (BL-tag) with low molecular weight fluorogenic β-lactam probes. The study concerned FRET to optimize the emission of the probe. A shortcoming of the strategy involved the suitable choice of donor fluorophore, acceptor quencher and their application in physiological conditions. To surmount the restraint in the FRET process, our new approach is based on the switching mechanism involving aggregation followed by elimination processes. In the modified version, the quenching ability of the fluorescence quencher does not depend upon the emission wavelength of the fluorophore, as is desired for an effective FRET process. In this case the quenching phenomenon is the intrinsic property of the quencher part.

We have continued our study with the same BL-tag protein. The reaction of TEM-1 (class A β-lactamases) with β-lactam rings involves acylation and deacylation steps. Glu166 is indispensable for the deacylation step,[11] and the mutant version of TEM-1 (^{E166N}TEM or BL) restricts the deacylation step.[12] Our aim was to exploit the properties of BL for covalent attachment with a fluorescent substrate with a better versatile technique. Here, we present a rationally designed fluorogenic probe that takes advantage of the aggregation of fluorophore and quencher. In the aggregated form, the interaction between the fluorogenic part and the quencher restricts the emission of the fluorophore. The viability of the fluorescently labeled BL-tag under physiological situations has been explored with the newly designed and synthesized a cephalosporin-based fluorescent probe (**FCDNB**, Scheme 1a). We have used the *m*-dinitrobenzene (DNB) group as quencher, whose quenching efficiency is well established.[13] The probe contains 6-carboxyfluorescein as fluorophore and DNB as quencher and they are connected to different sides of the β-lactam ring of the central cephalosporin part. A flexible spacer can control the emission[14] and enzyme activity prompts

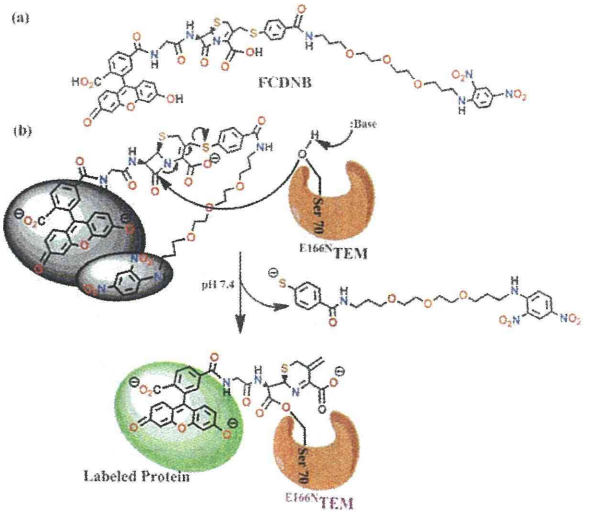

Scheme 1 Labeling strategy with (a) structure and (b) labeling state of the fluorescent probe **FCDNB**.

[a] *Division of Advanced Science and Biotechnology, Graduate School of Engineering, Osaka University, 2-1 Yamadaoka, Suita, Osaka 565-0871, Japan. E-mail: kkikuchi@mls.eng.osaka-u.ac.jp; Fax: (+81) 6-6879-7875*
[b] *Immunology Frontier Research Center, Osaka University, 2-1 Yamadaoka, Suita, Osaka 565-0871, Japan*

† Electronic supplementary information (ESI) available: Experimental details, chemical structures, UV-Visible absorption spectra, and fluorescence spectra of **FCDNB**. See DOI: 10.1039/c0cc02432e

the fluorescence recovery. This inspired us to introduce polyethylene glycol in the newly developed system for better aggregation interaction and solubility in physiological conditions. Incubation with BL-tag protein leads to the subsequent elimination of quencher to label the covalent modification of the tag protein with the desired fluorophore. Using this modification, we can achieve a new and better route to a turn-on fluorescence protein labeling system compared to our previous FRET analogue under the same physiological conditions. The advantage of this design principle is robustness towards fluorescein, whose fluorescence intensity was not easily modified by the previous design,[10] since the quenching mechanism is due to simple molecular interactions.

The labeling mechanism is illustrated in Scheme 1b. Cleavage of the β-lactam group of **FCDNB** by Ser70 in BL produced covalent labeling of the fluorescein to the protein with concomitant release of DNB. The labeled protein was detected by irradiating the gel with visible light (λ = 470 nm) in an SDS-PAGE study. A protein band of ~29 kDa was observed, exhibiting green fluorescence (Fig. 1a). To confirm that the labeling activity is due to the BL-tag, we carried out a similar experiment with wild-type (WT) TEM-1. In contrast to BL, incubation of WT TEM with **FCDNB** ended with no labeled fluorescence. Labeling in a biological medium with HEK293T cell lysate was also checked. SDS-PAGE analysis confirmed competent and selective labeling of **FCDNB** (Fig. 1b).

Compound **8** (Fig. S2†) with only DNB quencher showed maximum absorption at 364 nm and negligible absorption after 475 nm in HEPES buffer, whereas there is no substantial emission of fluorescein in this region (Fig. S3†). The probability of FRET from fluorescein to the DNB group can be overruled due to the insignificant overlap of fluorescein emission and DNB absorbance. The absorption peaks of fluorescein and the DNB group in **FCDNB** were obtained at 507 nm and 375 nm, respectively, in HEPES buffer. In methanol, the absorption peaks for both fluorescein and DNB were shifted by 10–15 nm (Fig. S4†). These positional shifts suggest a different nature of interaction between the fluorophore and quencher in the studied media.

The fluorescence quantum yield of **FCDNB** was found to be 0.05 in 100 mM HEPES buffer. This result confirmed that the

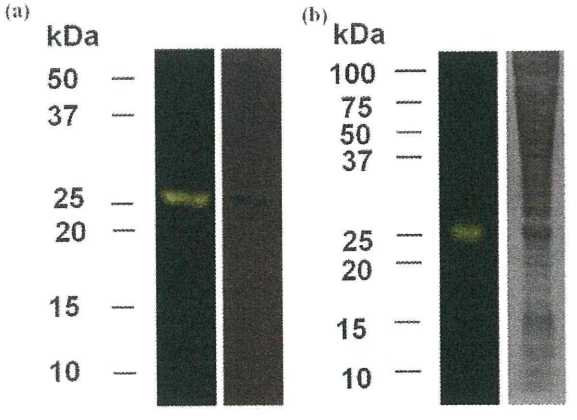

Fig. 1 **FCDNB** incubated fluorescence (left) and CBB-stained (right) gel images of (a) BL and (b) BL mixed with HEK293T cell lysate.

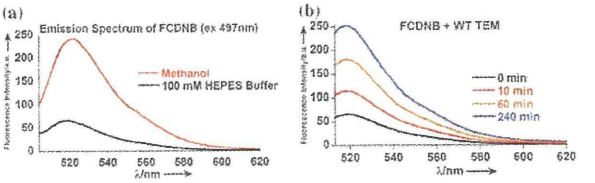

Fig. 2 (a) Emission spectra of **FCDNB** in 100 mM HEPES buffer (pH 7.4) and methanol (conc. of **FCDNB** 0.5 μM). (b) Time-dependent emission spectra (λ_{ex} = 507 nm) of **FCDNB** in the presence of WT TEM in 100 mM HEPES buffer (pH 7.4) containing 0.05% DMSO at 25 °C.

fluorescein emission was sufficiently quenched because of intramolecular interaction between the fluorophore and DNB group. 2,4-Dinitroaniline is an efficient intramolecular fluorescence quencher for fluorescein labeled oligonucleotides.[15] The mechanism of fluorescence attenuation can be attributed to electron-rich aromatic rings that can π-stack with the electron-poor nitroaromatics.[16] The inherent quenching phenomenon of DNB does not depend upon the nature of fluorophores, rather it has been found effective in the case of several fluorogenic probes.[17] The quantum yield of **FCDNB** in methanol is 0.42. This significant difference of emissions in these two solutions (Fig. 2a) implies that the aggregation phenomenon is favorable in the physiological conditions only. Buffer comparison studies of **FCDNB** and the DNB-free version of the probe (**FA**, Fig. S5†) showed that **FCDNB** is sufficiently quenched in each buffer medium (Table S1†). A pH probe fluorescence assay of **FCDNB** (Fig. S6†) suggests that emission from fluorescein is more effective at physiological conditions compared to in acidic medium.

The effects of BL-tag and WT TEM on the emission properties of the probe were studied. The fluorescence intensity at 520 nm due to fluorescein was monitored after the incubation of BL with **FCDNB**. Slow enhancement of the fluorescence intensity was observed with time (Fig. S7†). This indicates that the cleavage of the β-lactam of **FCDNB** was performed by BL but the disaggregation followed by elimination of the DNB group is very slow. The process is significantly different in case of the incubation study with WT TEM. The DNB group was eliminated by WT TEM with a much faster rate and the fluorescence signal increased a considerable amount (Fig. 2b) as expected due to the favorable deacylation step of the catalytic activity. The change in fluorescence enhancement was found to be slow after 4 h. The initial rate of fluorescence enhancement in the case of WT TEM was found to be ~20 times that of the BL-tag. This noticeable difference in the rate of reaction is also due to the controlled acylation path as a result of mutation at Glu166.[10] In comparison, emission intensities of fluorescein in **FA** remain the same with time for both WT TEM and BL-tag.

The site-specific labeling of target proteins has been probed by the demonstration of **FCDNB** on the surface of living cells (Fig. 3a). For this purpose we have chosen the N-terminus of epidermal growth factor receptor (EGFR). The target fluorophore recognizes the transfected protein as a result of covalent bond formation. The BL-tag fused to the EGFR, and then it was expressed with HEK293T cells. After treatment with **FCDNB**, fluorescence images of the HEK293T cells were

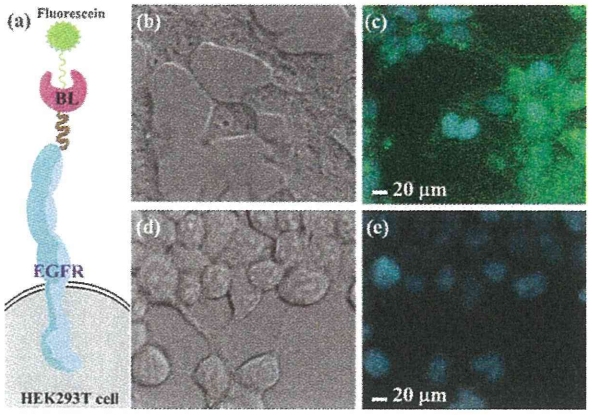

Fig. 3 (a) Labeling of protein with the probe through the BL-tag. (b)–(e) Optical microscopic images of **FCDNB**-labeled HEK293T cells expressing (b,c) BL-EGFR and (d,e) EGFR. (b,d) DIC images, (c,e) fluorescence microscopic images. The cell nuclei were stained with Hoechst 33342. For fluorescence microscope images, the cells were excited at 330–385 nm for Hoechst 33342, and 460–490 nm for **FCDNB**.

taken under an inverted fluorescence microscope. The cell nuclei were stained with Hoechst 33342. Only the cells expressing the BL-EGFR fusion protein emitted green fluorescence as a consequence of specific labeling by the probe (Fig. 3c). In the case of HEK293T cells expressing the EGFR protein without any BL-tag, the cell nuclei show only cyan fluorescence due to Hoechst 33342. In this case no fluorescein-labeled cell was observed (Fig. 3e).

In conclusion, we have modified our protein labeling method with an improved and straightforward technique that merges a BL-tag with a low molecular weight fluorogenic β-lactam probe. Through appropriate modification of our probe design, we succeeded in labeling targeted proteins with a familiar and useful fluorophore *in vitro* and also in living cells. Despite the similarity in molecular weight of the BL and Green Fluorescent Protein (GFP), fluorogenicity can be introduced through BL-tag technology, which is rather impossible with GFP. In this tailored version, the system can be considered as preliminary proof of a newly developed principle. By introducing a more efficiently quenched probe, this system can solve the problem of washing procedures after the labeling method. We are presently engaged in the aspect of the versatile use of this customized *modus operandi* with a range of fluorophores.

This research is supported by the Japan Society for the Promotion of Science (JSPS) through its "Funding Program for World-Leading Innovative R&D on Science and Technology (FIRST Program). This work was supported in part by the Grant-in-Aid for Scientific Research from the Ministry of Education, Culture, Sports, Science and Technology (MEXT) of Japan, the Grant-in-Aid from the Ministry of Health, Labour and Welfare (MHLW) of Japan, and the New Energy and Industrial Technology Development Organization (NEDO) of Japan. KK expresses his special thanks for support from the Takeda Science Foundation. KKS and SW acknowledge support from a Global COE Fellowship of Osaka University. SW acknowledges JSPS Research Fellowship.

Notes and references

1 L. W. Miller and V. W. Cornish, *Curr. Opin. Chem. Biol.*, 2005, **9**, 56.
2 (*a*) P. I. H. Bastiaens and T. M. Jovin, *Proc. Natl. Acad. Sci. U. S. A.*, 1996, **93**, 8407; (*b*) J. Yin, F. Liu, X. Li and C. T. Walsh, *J. Am. Chem. Soc.*, 2004, **126**, 7754; (*c*) I. Chen, M. Howarth, W. Lin and A. Y. Ting, *Nat. Methods*, 2005, **2**, 99; (*d*) L. W. Miller, Y. Cai, M. P. Sheetz and V. W. Cornish, *Nat. Methods*, 2005, **2**, 255; (*e*) G. Ulrich, C. Goze, M. Guardigli, A. Roda and R. Ziessel, *Angew. Chem., Int. Ed.*, 2005, **44**, 3694; (*f*) R. McRae, B. Lai, S. Vogt and C. J. Fahrni, *J. Struct. Biol.*, 2006, **155**, 22; (*g*) H.-K. Kim, J. Liu, J. Li, N. Nagraj, M. Li, C. M.-B. Pavot and Y. Lu, *J. Am. Chem. Soc.*, 2007, **129**, 6896; (*h*) B. Li, H. Wei and S. Dong, *Chem. Commun.*, 2007, 73; (*i*) B. C. Dickinson and C. J. Chang, *J. Am. Chem. Soc.*, 2008, **130**, 9638; (*j*) M. A. Brun, K.-T. Tan, E. Nakata, M. J. Hinner and K. Johnsson, *J. Am. Chem. Soc.*, 2009, **131**, 5873; (*k*) H. Ren, F. Xiao, K. Zhan, Y.-P. Kim, H. Xie, Z. Xia and J. Rao, *Angew. Chem., Int. Ed.*, 2009, **48**, 9658; (*l*) Y. Zou and J. Yin, *J. Am. Chem. Soc.*, 2009, **131**, 7548.
3 R. Y. Tsien, *Annu. Rev. Biochem.*, 1998, **67**, 509.
4 M. Fernandez-Suarez and A. Y. Ting, *Nat. Rev. Mol. Cell Biol.*, 2008, **9**, 929.
5 (*a*) B. A. Griffin, S. R. Adams and R. Y. Tsien, *Science*, 1998, **281**, 269; (*b*) C. Hoffmann, G. Gaietta, M. Bünemann, S. R. Adams, S. Oberdorff-Maass, B. Behr, J.-P. Vilardaga, R. Y. Tsien, M. H. Ellisman and M. J. Lohse, *Nat. Methods*, 2005, **2**, 171.
6 (*a*) A. Keppler, S. Gendreizig, T. Gronemeyer, H. Pick, H. Vogel and K. Johnsson, *Nat. Biotechnol.*, 2003, **21**, 86; (*b*) D. Maurel, S. Banala, T. Laroche and K. Johnsson, *ACS Chem. Biol.*, 2010, **5**, 507.
7 (*a*) H. Nonaka, S. Tsukiji, A. Ojida and I. Hamachi, *J. Am. Chem. Soc.*, 2007, **129**, 15777; (*b*) G. V. Los, L. P. Encell, M. G. McDougall, D. D. Hartzell, N. Karassina, C. Zimprich, M. G. Wood, R. Learish, R. F. Ohana, M. Urh, D. Simpson, J. Mendez, K. Zimmerman, P. Otto, G. Vidugiris, J. Zhu, A. Darzins, D. H. Klaubert, R. F. Bulleit and K. V. Wood, *ACS Chem. Biol.*, 2008, **3**, 373.
8 (*a*) M. W. Popp, J. M. Antos, G. M. Grotenbreg, E. Spooner and H. L. Ploegh, *Nat. Chem. Biol.*, 2007, **3**, 707; (*b*) H. Baruah, S. Puthenveetil, Y. A. Choi, S. Shah and A. Y. Ting, *Angew. Chem., Int. Ed.*, 2008, **47**, 7018.
9 H. Kobayashi, M. Ogawa, R. Alford, P. L. Choyke and Y. Urano, *Chem. Rev.*, 2010, **110**, 2620.
10 S. Mizukami, S. Watanabe, Y. Hori and K. Kikuchi, *J. Am. Chem. Soc.*, 2009, **131**, 5016.
11 G. Guillaume, M. Vanhove, J. Lamotte-Brasseur, P. Ledent, M. Jamin, B. Joris and J.-M. Frére, *J. Biol. Chem.*, 1997, **272**, 5438.
12 H. Adachi, T. Ohta and H. Matsuzawa, *J. Biol. Chem.*, 1991, **266**, 3186.
13 R. Livingston, L. Thompson and M. V. Ramarao, *J. Am. Chem. Soc.*, 1952, **74**, 1073.
14 Y. Hori, H. Ueno, S. Mizukami and K. Kikuchi, *J. Am. Chem. Soc.*, 2009, **131**, 16610.
15 T. Maier and W. Pfleiderer, *Nucleosides, Nucleotides Nucleic Acids*, 1995, **14**, 961.
16 (*a*) M. E. Germain, T. R. Vargo, B. A. McClure, J. J. Rack, P. G. Van Patten, M. Odoi and M. J. Knapp, *Inorg. Chem.*, 2008, **47**, 6203; (*b*) J.-S. Yang and T. M. Swager, *J. Am. Chem. Soc.*, 1998, **120**, 5321.
17 (*a*) E. L. Kapinus and I. I. Dilung, *Chem. Phys. Lett.*, 1990, **174**, 75; (*b*) K.-S. Focsaneanu and J. C. Scaiano, *Photochem. Photobiol. Sci.*, 2005, **4**, 817; (*c*) H. Li, J. Kang, L. Ding, F. Lu and Y. Fang, *J. Photochem. Photobiol., A*, 2008, **197**, 226.

Multicolor Protein Labeling in Living Cells Using Mutant β-Lactamase-Tag Technology

Shuji Watanabe,[†] Shin Mizukami,[†,‡] Yuichiro Hori,[†] and Kazuya Kikuchi*[,†,‡]

Division of Advanced Science and Biotechnology, Graduate School of Engineering, and Immunology Frontier Research Center, Osaka University, 2-1 Yamadaoka, Suita, Osaka, 565-0871, Japan. Received July 29, 2010; Revised Manuscript Received September 21, 2010

Protein labeling techniques using small molecule probes have become important as practical alternatives to the use of fluorescent proteins (FPs) in live cell imaging. These labeling techniques can be applied to more sophisticated fluorescence imaging studies such as pulse-chase imaging. Previously, we reported a novel protein labeling system based on the combination of a mutant β-lactamase (BL-tag) with coumarin-derivatized probes and its application to specific protein labeling on cell membranes. In this paper, we demonstrated the broad applicability of our BL-tag technology to live cell imaging by the development of a series of fluorescence labeling probes for this technology, and the examination of the functions of target proteins. These new probes have a fluorescein or rhodamine chromophore, each of which provides enhanced photophysical properties relative to coumarins for the purpose of cellular imaging. These probes were used to specifically label the BL-tag protein and could be used with other small molecule fluorescent probes. Simultaneous labeling using our new probes with another protein labeling technology was found to be effective. In addition, it was also confirmed that this technology has a low interference with respect to the functions of target proteins in comparison to GFP. Highly specific and fast covalent labeling properties of this labeling technology is expected to provide robust tools for investigating protein functions in living cells, and future applications can be improved by combining the BL-tag technology with conventional imaging techniques. The combination of probe synthesis and molecular biology techniques provides the advantages of both techniques and can enable the design of experiments that cannot currently be performed using existing tools.

INTRODUCTION

Recent prominent advances in fluorescence imaging techniques enabled investigations of direct localization and trafficking of biomolecules in living cells. Genetic engineering has also been progressing dramatically and provides methods for expressing various proteins in specific organelles in cells. Fusion proteins prepared by linkage of fluorescent proteins (FPs) can be used to obtain tools for imaging any protein of interest (POI) (*1*). However, it is difficult to use FPs in pulse-chase imaging studies for investigating protein function over time within the space inside a living cell and to optimize fluorescence properties such as emission and excitation wavelengths, extinction coefficients, and photostability for various experiments. Moreover, certain FPs tend to form protein aggregates that affect the function and/or localization of the target POIs (*2, 3*).

Protein labeling methods using small molecule probes have attracted great attention because they may have the ability to overcome the limitations of FPs. Several methods for labeling proteins with small molecules have been commercialized, including Lumio-tag (*4*−*6*), HaloTag (*7*), SNAP-tag (*8*−*10*), and DHFR-based tag (*11*). Lumio-tag, using FlAsH or ReAsH, is based upon a fluorescent biarsenical dye that reacts with tetracysteine peptide and generates strong fluorescence. HaloTag is a modified haloalkane dehalogenase designed to covalently react with synthetic haloalkyl ligands. SNAP-tag utilizes human O^6-alkylguanine-DNA-alkyltransferase (hAGT) as the protein tagged with synthetic benzylguanine derivatives. DHFR-based tag employs the noncovalent interaction between *Escherichia coli* dihydrofolate reductase and fluorescently labeled methotrexate. Other protein labeling methods based on biotin ligase (*12*), transglutaminase (*13*), hexahistidine (*14*), and tetraaspartic acid (*15*) have also been reported.

The advantages of synthetic fluorescent probes are tunable switches for changes in fluorescence characteristics. These probes have intense fluorescence properties and provide a wide range of choices in fluorophores. Meanwhile, the advantages of using protein expression systems are provided by specific expression in cellular components and tissues, convenient experimental procedures, and the potential for in vivo studies using transgenic mice. Combining the advantages of both techniques is expected to provide enhanced methods for exploring molecular functions in biological systems.

For incorporation of the tunable switches in expressed protein tags, we previously reported a specific protein labeling system with an off/on fluorescence switch that employs a mutant enzyme and its specific substrate. The system involves covalent modification of a mutant β-lactamase (BL-tag) with a rationally designed fluorogenic probe based on fluorescence resonance energy transfer (FRET) (*16*). β-Lactamases are members of a family of bacterial enzymes that efficiently cleave β-lactam moieties within compounds such as penicillins and cephalosporins (*17*). Since the activity of β-lactamases is not observed in eukaryotic cells, these proteins have been widely exploited as reporter enzymes in living mammalian cells (*18*−*20*). Furthermore, their three-dimensional structures, catalytic mechanism, and inhibitors have been widely studied because of their clinical importance (*21*). A well-characterized isoform is the 29 kDa TEM-1 β-lactamase from *Escherichia coli* categorized as a class A β-lactamase (*22*).

* E-mail: kkikuchi@mls.eng.osaka-u.ac.jp. Phone: +81-6-6879-7924. Fax: +81-6-6879-7875.
[†] Division of Advanced Science and Biotechnology.
[‡] Immunology Frontier Research Center.

10.1021/bc100333k
Published on Web 10/20/2010

Scheme 1. Reaction Mechanism of Wild-Type (WT) and Mutant (E166N) TEM-1 β-Lactamase

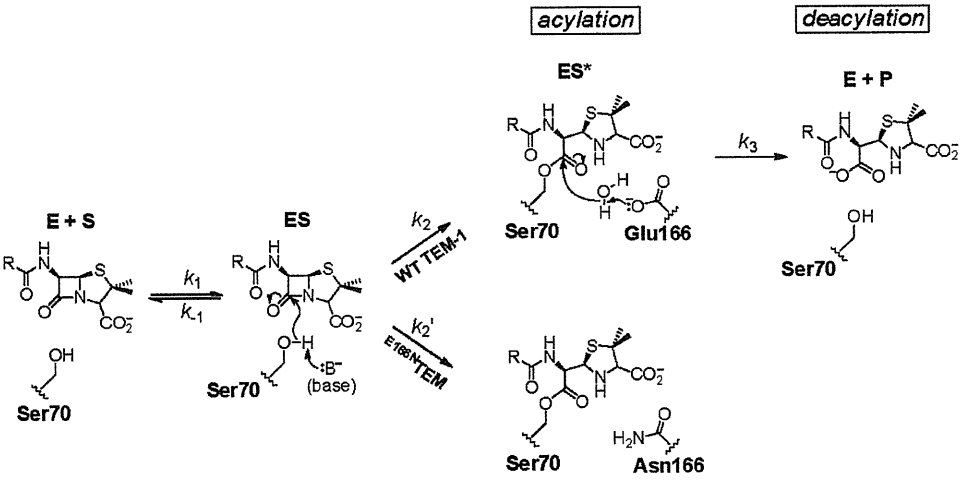

The reaction of wild-type (WT) TEM-1 with β-lactams involves acylation and deacylation steps (Scheme 1). Nucleophilic attack on the β-lactam ring by Ser70 leads to the covalent acyl-enzyme intermediate. In WT TEM-1, Glu166 acts as a base to catalyze hydrolysis of the intermediate (*23*), resulting in release of the product and regeneration of WT TEM-1. In ^{E166N}TEM, Asn166 is ineffective as a base; hence, the intermediate accumulates as a stable covalent adduct (*24*).

According to the above-mentioned mechanism, we have reported a novel protein labeling system with an off−on fluorescence switch based on a combination of a mutant β-lactamase (BL-tag) and coumarin-based substrates. Owing to the rational design of both the tag protein and the labeling probes, this system enabled us to simultaneously achieve specific and fluorogenic labeling of the target protein on living cells (*16*). In our previous report, we designed and synthesized both a simple fluorescent labeling probe, designated CA, and a fluorogenic probe, designated CCD. CA is a 7-hydroxycoumarin−ampicillin conjugate and CCD includes three main components; 7-hydroxycoumarin, cephalosporin, and DABCYL. The fluorescence of CCD is largely quenched by intramolecular FRET from coumarin to DABCYL. Cleavage of the cephalosporin β-lactam ring produces a free amino group, which triggers spontaneous elimination of any leaving group previously attached to the 3′ position (*25*). Consequently, fluorogenic labeling with CCD of fusion proteins of ^{E166N}TEM (BL-tag) was successfully performed in vitro and on the surfaces of living cells.

In this paper, we demonstrated the broad applicability of this labeling technology for live cell imaging experiments by developing a series of labeling probes with various fluorophores. We also show that this technology has a low interference with respect to the functions of EGFR and is orthogonal to another currently used protein labeling method.

EXPERIMENTAL PROCEDURES

Fluorometric Analysis. The slit width was 2.5 nm for both excitation and emission, and the photomultiplier voltage was 700 V. All fluorescent probes were dissolved in DMSO to obtain 10 mM stock solutions, and these solutions were diluted to the desired final concentrations with an appropriate aqueous buffer solution. Relative fluorescence quantum yields of the compounds were obtained by comparing the area under the emission spectrum of the sample with that of an EtOH solution of rhodamine B, which has a quantum efficiency of 0.97 when excited at 545 nm (*26*), and with that of a 100 mM NaOH solution of fluorescein, which has a quantum efficiency of 0.85 when excited at 492 nm (*27*).

Calculation of Förster Distance (R_0) and Energy Transfer Efficiency (E). For evaluation of R_0 and E, a revised version of the Förster formula was used (*28*)

$$R_0 = 9.78 \times 10^3(\Phi_D \kappa^2 n^{-4} J)^{1/6} \quad \left(J = \int_0^\infty f_D(\lambda)\varepsilon_A \lambda^4 \, d\lambda\right)$$

$$E = R_0^6/(R_0^6 + R^6)$$

where R_0 is expressed in Å units, κ^2 is the orientation factor, Φ_D is the donor quantum yield in the absence of acceptor, n is the refractive index of the medium, $f_D(\lambda)$ is the normalized donor emission spectrum, $\varepsilon_A(\lambda)$ is the acceptor molar absorption coefficient in M^{-1} cm^{-1} units, and R is the donor−acceptor distance. The wavelength is expressed in nanometer units. The value $\kappa^2 = 2/3$, which corresponds to a dynamic isotropic regime, was assumed and $n = 1.33$ was applied. The molar absorption coefficient (ε) of DABCYL was 25 500 ($\lambda = 462$ nm) in 100 mM HEPES buffer (pH 7.4). R_0 values were calculated for the CA-DABCYL pair for CCD, the FA-DABCYL pair for FCD, and the RA-DABCYL pair for RCD. The quantum yields (Φ_D) of the compounds were 0.40 for CA, 0.71 for FA, and 0.49 for RA. The donor−acceptor distance (R) was evaluated by using the integrated molecular modeling packages *Maestro* v 8.5 and *MacroModel* v 9.6.

HPLC Analysis. HPLC analyses were performed with an Inertsil ODS-3 (4.6 × 250 mm) column (GL Sciences Inc.) using an HPLC system that comprises a pump (PU-2080, JASCO) and a detector (MD-2010 or FP-2020, JASCO). Preparative HPLC was performed with an Inertsil ODS-3 (10.0 × 250 mm) column (GL Sciences Inc.) using an HPLC system that comprises a pump (PU-2087, JASCO) and a detector (UV-2075, JASCO).

Fluorescence Microscopy. Fluorescence microscopic images were recorded using a IX71 fluorescence microscope (Olympus), a Cool Snap HQ cooled CCD camera (Roper Scientific), and a USH-103OL mercury lamp (Olympus). The filter sets used were Olympus BP330-385, DM455, and BA455 for Hoechst 33342 and coumarin derivatives; BP470-495, DM505, and BA510-550 for fluorescein derivatives; and BP510-550, DM575, and BA575-625 for rhodamine derivatives. *MetaMorph* imaging software (Universal Imaging Corporation) was used for imaging and data analysis.

Detection of Protein Labeling by SDS-PAGE. WT TEM-1 or ^{E166N}TEM (*16*) (20 μM) was added to a solution of probes (30 μM) in 100 mM HEPES buffer (pH 7.4) at 25 °C. After 30 min, the labeled protein was denatured in 2 × SDS gel loading buffer (100 mM Tris−HCl buffer (pH 6.8), 2.5% SDS, 20%

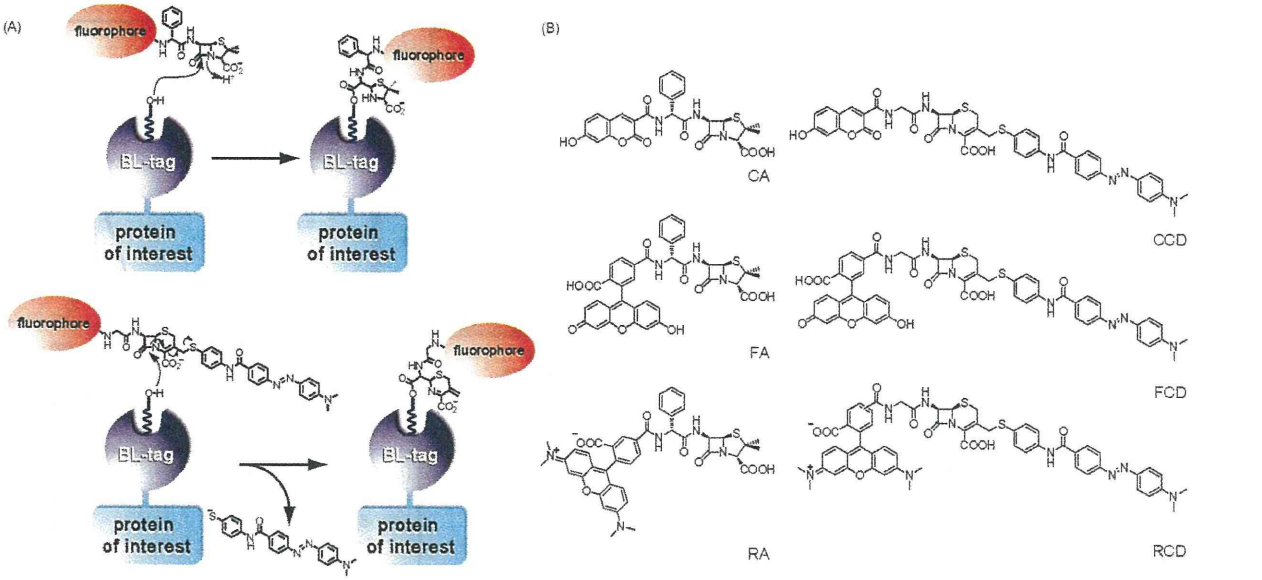

Figure 1. (A) General labeling mechanisms of the ampicillin- and cephalosporin-based probes. (B) Structures of β-lactam derivatives used for fluorescence labeling of BL-tag fusion proteins.

glycerol, and 10% mercaptoethanol) and resolved by NuPAGE (12% bis-Tris gel, Invitrogen). The fluorescence images of the gels were captured using a digital camera (Nikon COOLPIX P6000). The gels were stained with Coomassie Brilliant Blue prior to the capture of images.

Labeling of Cell Surface pcDNA3.1(+)-^{E166N}TEM-EGFR (BL-EGFR) with Various Probes. HEK293T cells maintained in 10% FBS in DMEM (Invitrogen) at 37 °C under 5% CO_2 were transfected with a plasmid coding for BL-EGFR, which was prepared as described previously (*16*), using Lipofectamine 2000 (Invitrogen). After 5−6 h, the culture medium was replaced with DMEM (without phenol red), and the cells were incubated at 37 °C for 24 h. The cells were then washed three times with DMEM (without phenol red) and incubated with 10 μM labeling probes in a CO_2 incubator for 30 min for CA, FA, and RA, or for 2 h for CCD and FCD. The cell nuclei were co-stained with Hoechst 33342 (100 ng mL^{-1}). After washing with DMEM containing 10% FBS, cells were incubated with HBSS, and the fluorescence images were captured with appropriate filter sets for each of the fluorophores.

Analysis of Fluorescence Images. Labeled cell images with CA, CCD, FA, and RA were acquired according to the above-mentioned procedure. 256 × 256 pixels area, where cells were confluently cultured, was selected at random from the acquired fluorescence images. The average fluorescence intensity of different colors per pixel was computed from the selected area using *MetaMorph* imaging software.

Multilabeling of Cells with BL-tag and SNAP-tag. Plasmids coding for BL-EGFR and COX8-2-SNAP were co-transfected into HEK293T cells. The cells were then incubated with FA, SNAP-Cell TMR Star, and Hoechst 33342 in a CO_2 incubator for 30 min (final concn of FA, 10 μM; SNAP-Cell TMR Star, 0.8 μM; Hoechst 33342, 100 ng mL^{-1}), and the fluorescence images were captured. The detailed procedure was the same as the procedure followed for the single protein labeling.

Western Blot Analysis of EGFR and BL-EGFR Expressed in HEK293T Cells after EGF Stimulation. HEK293T cells were transfected with BL-EGFR or pcDNA3.1(+)-EGFR using Lipofectamine 2000. After 5−6 h, the culture medium was replaced with DMEM, and the cells were incubated at 37 °C for 24 h. Prior to EGF addition, the cells were incubated overnight in the medium containing 0.5% serum. The cells were then washed once with PBS (−) and treated with EGF (100 ng mL^{-1}, Sigma, E9644) for 10 min at 25 °C. After one rinse with PBS (−), the cells were lysed with 200 μL of 1× SDS gel loading buffer (50 mM Tris−HCl buffer (pH 6.8), 1.3% SDS, 10% glycerol, and 5% mercaptoethanol). After scraping, the lysates were boiled at 95 °C for 3 min. Subsequently, samples were electrophoresed in a 7.5% or 10% SDS-polyacrylamide gel and transferred to PVDF membranes for Western blot. Membranes were blocked by 1 h incubation with TBST buffer (0.01% Tween 20, 138 mM NaCl, 20 mM Tris, pH 7.6) containing 5% skim milk (for anti-EGFR, anti-β-lactamase, and anti-β-actin antibodies) or 3% BSA (for anti-EGFR-pY1197 antibody) at room temperature. Then, anti-EGFR (1:500 dilution), anti-β-lactamase (1:5000 dilution), anti-EGFR-pY1197 (1:500 dilution), or anti-β-actin (1:5000 dilution) antibodies were added to each membrane. After incubation for 16 h at 4 °C with shaking, the membranes were washed three times with TBST buffer, incubated with horseradish peroxidase-linked secondary antibody, washed with TBST buffer, and visualized using ECL Western blotting detection reagents.

Immunofluorescence Detection of the Tyrosine Phosphorylation on BL-EGFR after EGF Stimulation. Transfected HEK293T cells were prepared and treated with EGF according to the above-mentioned procedure. After one rinse with PBS(−), the cells were fixed with 3.7% formaldehyde/PBS(−) at 25 °C for 20 min. After two rinses with PBS(−), the cells were blocked with blocking buffer (PBS containing 5% Goat Serum (Invitrogen) and 0.05% NaN_3) at 25 °C for 1 h. Anti-EGFR-pY1197 antibody, followed by fluorescein-conjugated goat antimouse antibody, was used to stain BL-EGFR or EGFR. After mounting, microscopic images were acquired using a filter set for fluorescein.

RESULTS AND DISCUSSION

Design and Synthesis of Fluorophores for the Labeling of BL-tag Fusion Proteins. Although it was previously shown that BL-tag fusion proteins can be specifically labeled with 7-hydroxycoumarin-conjugated β-lactam probes (Figure 1), the fluorescence was found to be dim and the excitation wavelength was short and hindered by the intrinsic autofluorescence of mammalian cells. The use of brighter and longer-excitation wavelength fluorophores is advantageous for various functional

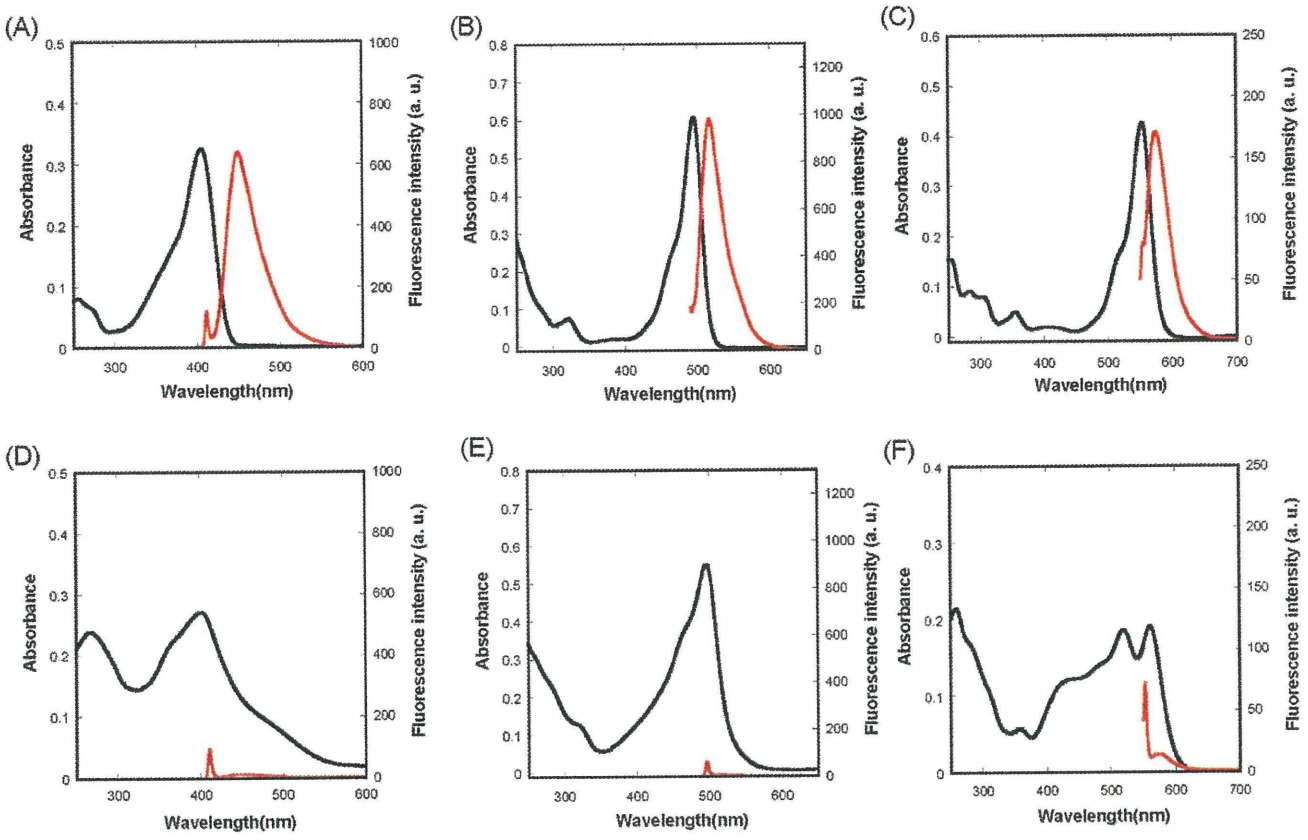

Figure 2. Absorption (black line) and emission spectra (red line) of (A) CA, (B) FA, (C) RA, (D) CCD, (E) FCD, and (F) RCD in 100 mM HEPES buffer (pH 7.4). In the absorption measurements, the probe concentrations were 5 μM for FA, FCD, RA, and RCD and 10 μM for CA and CCD. In the absorption measurements, the probe concentrations were 0.5 μM for FA, FCD, RA, and RCD and 1 μM for CA and CCD. Excitation wavelengths were 405 nm for CA and CCD, 492 nm for FA, 496 nm for FCD, and 553 nm for RA and RCD.

Table 1. Spectroscopic Properties and Calculated Values for FRET of Labeling Probes in 100 mM HEPES Buffer (pH 7.4)

compound	$\lambda_{abs,\ max}$/nm	$\lambda_{em,\ max}$/nm	fluorescence quantum efficiency (Φ)	Förester distance[a] (R_0)/Å	donor−acceptor distance[b] (R)/Å	energy transfer efficiency[c] (E)
CA	405	453	0.40	–	–	–
CCD	400	450	0.006	44.2	26.3	0.96
FA	492	517	0.71	–	–	–
FCD	496	520	0.005	43.4	27.8	0.93
RA	553	575	0.49	–	–	–
RCD	525, 565	573	0.07	19.6	27.7	0.12

[a] R_0 values were derived from the overlap integral between the absorption spectrum of DABCYL and the fluorescence spectrum of CA for CCD, FA for FCD, and RA for RCD. [b] R values were evaluated from the farthest distance between the fluorophore and DABCYL by using the molecular modeling software. [c] Energy transfer efficiencies were calculated from the equation $E = R_0^6/(R_0^6 + R^6)$.

studies using living cells. Therefore, β-lactam probes conjugated to fluorescein or tetramethylrhodamine (TAMRA) were designed and synthesized (Figure 1B). The fluorescence labeling probes FA and RA were synthesized in one step from ampicillin and activated esters of the corresponding fluorophores. FCD and RCD, which were designed to be fluorogenic as well as CCD, were also synthesized. RCD was synthesized from the activated ester of the 5(6)-TAMRA isomers and used for the experiments without separation of the 5(6)-isomers (see Figure S1 in Supporting Information).

Absorption and emission spectra of all β-lactam labeling probes are shown in Figure 2, and the spectroscopic properties are summarized in Table 1. FA and RA exhibited similar spectroscopic properties to fluorescein and TAMRA, respectively. From the Förster radii caluculated from their spectra and the simulated donor−acceptor distances, the FRET efficiency was estimated (Table 1). We predicted that FCD fluorescence would be quenched sufficiently from the FRET efficiency value. Indeed, FCD was largely quenched by intramolecular FRET from coumarin to DABCYL ($\Phi = 0.005$). In contrast, RCD fluorescence would theoretically not be quenched because of the limited overlap between the absorption spectrum of DABCYL and the emission spectrum of TAMRA. Nevertheless, RCD fluorescence was considerably quenched ($\Phi = 0.07$). This quenching of RCD fluorescence can be ascribed to the intramolecular association between TAMRA and DABCYL moieties. We previously reported that, if two hydrophobic dyes are located in close proximity, self-quenching occurs due to the close contact of the two dyes in aqueous solution (*29*). The fluorescence intensities of FCD and RCD were recovered by the addition of WT TEM-1 and BL-tag in a time-dependent manner (see Figure S2 in Supporting Information). These results indicate that elimination of the DABCYL moieties occurs by the enzymatic cleavage of the β-lactam in both cases. The labeling capabilities of all compounds with BL-tag were confirmed by SDS-PAGE (see Figure S3 in Supporting Information).

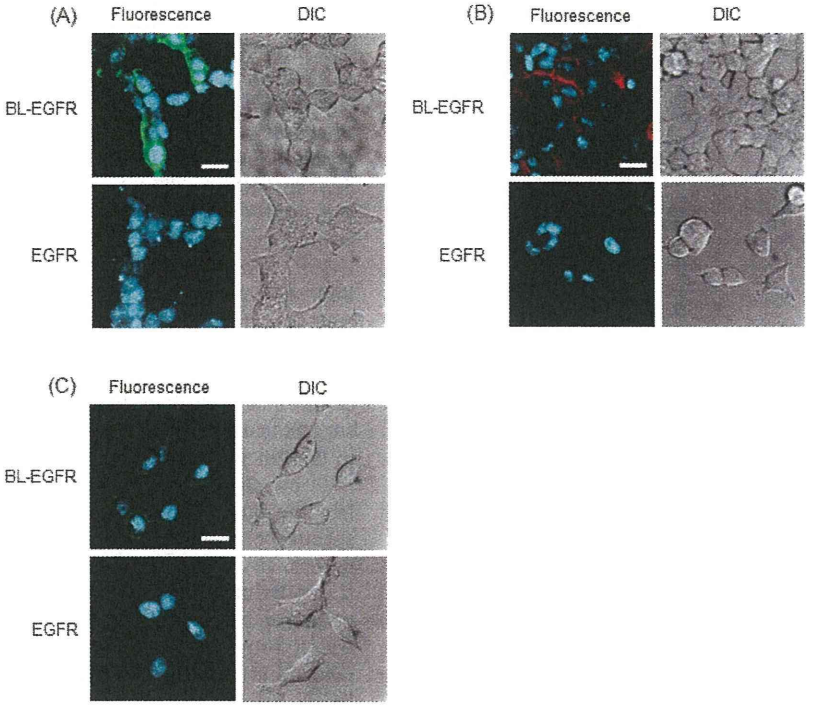

Figure 3. Labeling of BL-tag fusion proteins with (A) FA, (B) RA, and (C) FCD. HEK293T cells were transfected with a plasmid encoding BL-EGFR or EGFR. The cell nuclei were costained with Hoechst 33342. For fluorescence microscopic images, the cells were excited at 330−385 nm for Hoechst 33342, 460−490 nm for FA, and 510−550 nm for RA. Scale bar: 20 μm.

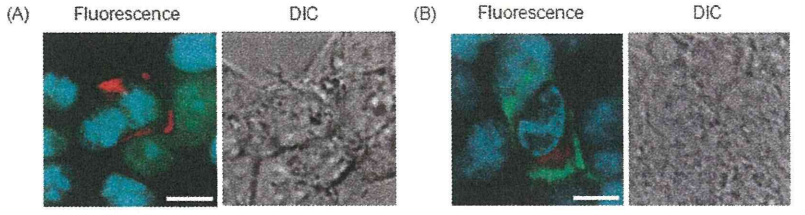

Figure 4. (A) Multicolor imaging of HEK293T cells expressing BL-EGFR. BL-EGFR, nuclei, and cytosol were labeled with RA (red), Hoechst 33342 (cyan), and CellTracker Green (green), respectively. (B) Multiprobe labeling of HEK293T cells expressing BL-EGFR and COX8-2-SNAP. BL-EGFR was labeled with FA, COX-8-2-SNAP with SNAP-Cell TMR-STAR, and nuclei with Hoechst 33342. Fluorescence microscopic images were excited at 330−385 nm, 460−490 nm, and 510−550 nm. Scale bar: 10 μm.

Fluorescence Labeling of BL-tag Fusion Proteins by the Synthesized Probes. BL-tag was fused to the N-terminus of epidermal growth factor receptor (EGFR), and the fusion protein BL-EGFR was expressed on cell surfaces of HEK293T cells by transfection with a plasmid encoding BL-EGFR. The cells were incubated with FA or RA, washed three times, and observed using a fluorescence microscope. The cells generating BL-EGFR clearly emitted green or red fluorescence at the plasma membrane (Figure 3A,B). We calculated the average fluorescence intensity per pixel from BL-EGFR expressing cells and negative control cells, and compared with each other (see Figure S4 in Supporting Information). As a result, the fluorescence signal from labeled cells by FA or RA was clearly enhanced compared with the background signal (about 1.8 times), while the fluorescence signal of cells labeled by CA or CCD was about 10% higher than the background signal. Therefore, the signal-to-background ratio was largely improved by FA and RA relative to CA and CCD. Subsequently, the labeling properties of FCD were investigated. The cells generating BL-EGFR were labeled by FCD in a labeling procedure similar to the procedure used for FA and RA (Figure 3C).

Multicolor Imaging by Simultaneous Labeling with BL-tag and SNAP-tag. We applied BL-tag technology to multicolor imaging of cells in order to demonstrate its wide versatility. After transfection of HEK293T cells with a plasmid encoding BL-EGFR, Hoechst 33342, CellTracker Green, and RA were incubated. Cells were then imaged using different fluorophores with appropriate filter sets. Each organelle was confirmed by multicolor fluorescence imaging (Figure 4A). In addition, BL-tag fusion proteins were found to be labeled with different color fluorophores (Figure 3). This property is beneficial for pulse-chase fluorescence imaging experiments used for tracing protein trafficking after various stimulations (*30, 31*).

Next, multicolor fluorescence labeling of two different target proteins was performed with another specific protein labeling system known as SNAP-tag technology. In this experiment, SNAP-tag was applied as a COX8-2-SNAP fusion plasmid encoding COX8-2 (subunit 8-2 protein of cytochrome c oxidase) cloned upstream of SNAP-tag. Cytochrome c oxidase is a terminal enzyme of the respiratory transport chain and localized at the inner mitochondrial membrane (*32*). The COX8-2-SNAP fusion proteins provide fluorescence in mitochondria when labeled with SNAP-Cell TMR-Star.

HEK293T cells were co-transfected with BL-EGFR and COX8-2-SNAP plasmids. The cells were incubated with FA, SNAP-Cell TMR-Star, and Hoechst 33342, and then washed three times with DMEM containing 10% FBS prior to imaging with a fluorescence microscope. Though the co-expression

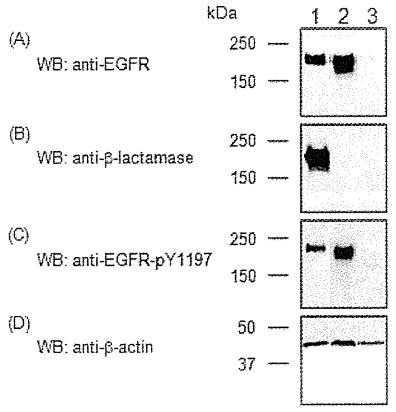

Figure 5. Western blot analysis of the EGFR and BL- EGFR expressed in transfected HEK293T cells after EGF stimulation. (A) Detection of EGFR with polyclonal anti-EGFR antibody. (B) Detection of TEM-1 with polyclonal anti-β-lactamase antibody. (C) Detection of phosphorylated tyrosine at 1197 position with monoclonal anti-EGFR-pY1197 antibody. (D) Detection of β-actin cytoskeleton with monoclonal anti-β-actin antibody. Lane 1: BL-EGFR-expressing cells. Lane 2: EGFR-expressing cells. Lane 3: Cells transfected with an empty plasmid vector.

efficiencies were not very good in this experiment, green fluorescence derived from FA was observed along the plasma membrane and red fluorescence from SNAP-Cell substrates in mitochondria was observed in the same cells (Figure 4B). This result distinctly indicates that BL-tag and SNAP-tag have nonoverlapping substrate specificity and can be used simultaneously in single cells.

Ligand-Induced Activation of the BL-tag Fusion Protein. Finally, we demonstrate the low interference of BL-tag with the function of the target protein EGFR. EGFR is a 170 kDa transmembrane glycoprotein that belongs to a tyrosine kinase receptor family comprising four members. The intracellular trafficking behavior and ligand-dependent dimerization of EGFR has attracted great attention (*33*). It was, however, reported that the expression and trafficking of EGFR was greatly disrupted as a result of extracellular GFP fusion and appropriate expression of the fusion protein was not detected by Western blot analysis with anti-GFP antibody (*34*) due to the fact that the fluorophore formation of GFP strongly depends upon the structural integrity of the protein (*3*). The identity of the BL-EGFR fusion protein was characterized by Western blot analysis with anti-β-lactamase, anti-EGFR, and anti-EGFR-pY1197 phosphorylation site-specific antibodies. Specific ligand binding on the extracellular domain of EGFR results in dimerization of the receptor and subsequent autophosphorylation of the tyrosine residues, the most predominant of which is pY1197 (*35*).

HEK293T cells were transfected with fusion proteins or EGFR plasmids, followed by incubation under serum-starved conditions. The cells were then stimulated with EGF and analyzed by Western blot. Naive (nontransfected) HEK293T cells express extremely low levels of endogenous EGFR as demonstrated in cells transfected with a control plasmid vector probed with an anti-EGFR antibody (lane 3 in Figure 5A) (*36*). When lysates of the cells transfected with EGFR plasmids were probed with an anti-EGFR antibody, one major band was visible with a molecular weight of about 170 kDa, corresponding to EGFR (lane 2 in Figure 5A). A single band was also detected from cells transfected with BL-EGFR. This band appeared in the slightly upper position of that of EGFR. This is consistent with the increase of the molecular weight as a result of fusion of BL-tag to EGFR (lane 1 in Figure 5A). On the other hand, when the membrane was probed with an anti-β-lactamase antibody, the immunoblotted band was observed only in the lane of the lysate containing BL-EGFR fusion protein (Figure 5B). These results suggest that the BL-EGFR fusion protein was properly expressed in HEK293T cells.

After stimulation by EGF, phosphorylation of Y1197 was confirmed using an anti-EGFR-pY1197 antibody. A single band shows that phosphorylation was observed in the lanes of cell lysates containing BL-EGFR or EGFR (lanes 1 and 2 in Figure 5C). In addition, we compared the distribution of BL-EGFR and EGFR after EGF stimulation by immunofluorescence staining with anti-EGFR-pY1197 antibody. Cells expressing BL-EGFR and EGFR gave the same distribution pattern of fluorescence responses that demonstrate phosphorylation in the cells (see Figure S5 in Supporting Information). From these results, it is evident that the phosphorylation function of EGFR can be preserved after introduction of the BL-tag to the extracellular domain of EGFR. All of the results discussed herein suggest that BL-tag has lower interference than GFP with respect to the function of EGFR.

In conclusion, we have designed and synthesized various labeling probes for BL-tag. These new probes have superior spectroscopic properties relative to the previously reported probes, CA and CCD. FA and RA can specifically label BL-tag in living cells, while FCD and RCD possess fluorogenic properties based on FRET or intramolecular stacking interaction which provides a useful switching mechanism for protein labeling probes, as we recently reported (*37*). The function of EGFR was found to be considerably preserved after the fusion of BL-tag to the extracellular domain. This low interference with the function of the target protein can provide a great advantage relative to fusion to GFP and should be suitable for studying the function or trafficking of POIs. Furthermore, BL-tag technology can be simultaneously used with other protein labeling methods such as SNAP-tag technology. Orthogonality of the substrate specificity between BL-tag and SNAP-tag was also shown.

In the future, a series of labeling probes with various fluorophores for BL-tag can be applied to a pulse-chase experiment that can distinguish between young and old copies of proteins by labeling at different time points with different fluorophores. Moreover, protein labeling techniques can be used not only for fluorescence imaging, but also for inducers of protein−protein interactions. Techniques based on multiple protein labeling methods are quite useful for studying and controlling protein−protein interactions (*38, 39*). Thus, we have provided a potential tool for practical biological applications. BL-tag technology can be exploited with conventional protein labeling methods for the specific labeling of two or more different proteins within a single cell. Furthermore, combinations of BL-tag technology with other imaging methods such as MRI or NIR are expected to contribute to the clarification of various protein−protein interactions.

ACKNOWLEDGMENT

This work was supported in part by the Grant-in-Aid for Scientific Research from the Ministry of Education, Culture, Sports, Science and Technology (MEXT) of Japan, by the Grant-in-Aid from the Ministry of Health, Labour and Welfare (MHLW) of Japan, and by the New Energy and Industrial Technology Development Organization (NEDO) of Japan. K.K. expresses his special thanks for support from the Takeda Science Foundation. S.W. acknowledges support from a Global COE Fellowship of Osaka University and a JSPS Research Fellowship.

Supporting Information Available: Materials and Instruments; synthetic details and characterization of FA, FCD, RA and RCD; supplementary figures. This material is available free of charge via the Internet at http://pubs.acs.org.

LITERATURE CITED

(1) Giepmans, B. N. G., Adams, S. R., Ellisman, M. H., and Tsien, R. Y. (2006) The fluorescent toolbox for assessing protein location and function. *Science 312*, 217–224.

(2) Phillips, G. N., Jr. (1997) Structure and dynamics of green fluorescent protein. *Curr. Opin. Struct. Biol. 7*, 821–827.

(3) Lisenbee, C. S., Karnic, S. K., and Trelease, R. T. (2003) Overexpression and mislocalization of a tail-anchored GFP redefines the identity of peroxisomal ER. *Traffic 4*, 491–501.

(4) Griffin, B. A., Adams, S. R., and Tsien, R. Y. (1998) Specific covalent labeling of recombinant protein molecules inside live cells. *Science 281*, 269–272.

(5) Griffin, B. A., Adams, S. R., Jones, J., and Tsien, R. Y. (2000) Fluorescent labeling of recombinant proteins in living cells with FLAsH. *Methods Enzymol. 327*, 565–578.

(6) Adams, S. R., Campbell, R. E., Gross, L. A., Martin, B. R., Walkup, G. K., Yao, Y., Llopis, J., and Tsien, R. Y. (2002) New biarsenical ligands and tetracystein motif for protein labeling *in vitro* and *in vivo*. Synthesis and biological applications. *J. Am. Chem. Soc. 124*, 6063–6076.

(7) Los, G. V., et al. (2008) Halotag: A novel protein labeling technology for cell imaging and protein analysis. *ACS Chem. Biol. 3*, 373–382.

(8) Keppler, A., Gendreizig, S., Pick, H., Vogel, H., and Johnsson, K. (2003) A general method for the covalent labeling of fusion proteins with small molecules *in vivo*. *Nat. Biotechnol. 21*, 86–89.

(9) Kindermann, M., Sielaff, I., and Johnsson, K. (2004) Synthesis and characterization of bifunctional probes for the specific labeling of fusion proteins. *Bioorg. Med. Chem. Lett. 14*, 2725–2728.

(10) Keppler, A., Pick, H., Arrivoli, C., Vogel, H., and Johnsson, K. (2004) Labeling of fusion proteins with synthetic fluorophores in live cells. *Proc. Natl. Acad. Sci. U.S.A. 101*, 9955–9959.

(11) Miller, L. W., Sable, J., Goelet, P., Sheetz, M. P., and Cornish, V. W. (2004) Methotrexate conjugates: A molecular *in vivo* protein tag. *Angew. Chem., Int. Ed. 43*, 1672–1675.

(12) Chen, I., Howarth, M., Lin, W., and Ting, A. Y. (2005) Site-specific labeling of cell surface proteins with biophysical probes using biotin ligase. *Nat. Methods 2*, 99–104.

(13) Lin, C.-W., and Ting, A. Y. (2006) Transglutaminase-catalyzed site-specific conjugation of small molecule probes to proteins *in vitro* and on the surface of living cells. *J. Am. Chem. Soc. 128*, 4542–4543.

(14) Hauser, C. T., and Tsien, R. Y. (2007) A hexahistidine-Zn^{2+}-dye label reveals STIM1 surface exposure. *Proc. Natl. Acad. Sci. U.S.A. 104*, 3693–3697.

(15) Ojida, A., Honda, K., Shinmi, D., Kiyonaka, S., Mori, Y., and Hamachi, I. (2006) Oligo-Asp tag/Zn(II) complex probe as a new pair for labeling and fluorescence imaging of proteins. *J. Am. Chem. Soc. 128*, 10452–10459.

(16) Mizukami, S., Watanabe, S., Hori, Y., and Kikuchi, K. (2009) Covalent protein labeling based on non-catalytic β-lactamase and a designed FRET substrate. *J. Am. Chem. Soc. 131*, 5016–5017.

(17) Christensen, H., Martin, T. M., and Waley, S. G. (1990) β-lactamase as fully efficient enzymes. *Biochem. J. 266*, 853–861.

(18) Moore, J. T., Davis, S. T., and Dev, K. I. (1997) The development of β-lactamase as a highly versatile genetic reporter for eukaryotic cells. *Anal. Biochem. 247*, 203–209.

(19) Zlokarnik, G., Negulescu, P. A., Knapp, T. E., Mere, L., Burres, N., Feng, L., Whitney, M., Roemer, K., and Tsien, R. Y. (1998) Quantitation of transcription and clonal selection of single living cells with β-lactamase as reporter. *Science 279*, 84–88.

(20) Gao, W., Xing, B., Tsien, R. Y., and Rao, J. (2003) Novel fluorogenic substrates for imaging β-lactamase gene expression. *J. Am. Chem. Soc. 125*, 11146–11147.

(21) Fisher, F. J., Meroueh, S. O., and Mobashery, S. (2005) Bacterial resistance to β-lactam antibiotics: Compelling opportunism, compelling opportunity. *Chem. Rev. 105*, 395–424.

(22) Matagne, A., Lamotte-Blasseur, J., and Frére, J.-M. (1998) Catalytic properties of class A β-lactamases: efficiency and diversity. *Biochem. J. 330*, 581–598.

(23) Guillaume, G., Vanhove, M., Lamotte-Brasseur, J., Ledent, P., Jamin, M., Joris, B., and Frére, J.-M. (1997) Site-directed mutagenesis of glutamate 166 in two β-lactamases. *J. Biol. Chem. 272*, 5438–5444.

(24) Adachi, H., Ohta, T., and Matsuzawa, H. (1991) Site-directed mutants, at position 166, of RTEM-1 β-lactamase that form a stable acyl-enzyme intermediate with penicillin. *J. Biol. Chem. 266*, 3186–3191.

(25) Page, M. I., and Proctor, P. (1984) Mechanism of β-lactam ring opening in cephalosporins. *J. Am. Chem. Soc. 106*, 3820–3825.

(26) Nishikawa, Y., and Hiraki, K. (1984) Calculation of quantum efficiency of rhodamine derivatives. *Analytical Methods of Fluorescence and Phosphorescence*, p 76, Kyoritsu Publishing Company, Tokyo

(27) Parker, C. A., and Rees, W. T. (1960) Correction of fluorescence spectra and measurement of fluorescence quantum efficiency. *Analyst 85*, 587–600.

(28) Lakowicz, J. R. (2006) Calculation of Förster distance and Energy transfer efficiency. *Principle of Fluorescence Spectroscopy*, 3rd ed., pp 443−475, Chapter 13, Springer Science+Business Media, LLV, New York.

(29) Mizukami, S., Kikuchi, K., Higuchi, T., Urano, Y., Mashima, T., Tsuruo, T., and Nagano, T. (1999) Imaging of caspase-3 activation in HeLa cells stimulated with etoposide using a novel fluorescent probe. *FEBS Lett. 453*, 356–360.

(30) Gaietta, G., Deerinck, T. J., Adams, S. R., Bouwer, J., Tour, O., Laird, D. W., Sosinsky, G. E., Tsien, R. Y., and Ellisman, M. H. (2002) Multicolor and electron microscopic imaging of connexin trafficking. *Science 296*, 503–507.

(31) Vivero-Pol, L., George, N., Krumm, H., Johnsson, K., and Johnsson, N. (2005) Multicolor imaging of cell surface proteins. *J. Am. Chem. Soc. 127*, 12770–12771.

(32) Malmström, B. G. (1990) Cytochrome c oxidase as a redox-linked proton pump. *Chem. Rev. 90*, 1247–1260.

(33) Sorkin, A., and Goh, L. K. (2009) Endocytosis and intracellular trafficking of ErbBs. *Exp. Cell Res. 315*, 683–696.

(34) Brock, R., Hamelers, I. H. L., and Jovin, T. M. (1999) Comparison of fixation protocols for adherent cultured cells applied to a GFP fusion protein of the epidermal growth factor receptor. *Cytometry 35*, 353–362.

(35) Chattopadhyay, A., Vecchi, M., Ji, Q., Memaugh, R., and Carpenter, G. (1999) The role of individual SH2 domain in mediating association of phospholipase C-γ1 with the activated EGF receptor. *J. Biol. Chem. 274*, 26091–26097.

(36) Jones, S. M., Foreman, S. K., Shank, B. B., and Kurten, R. C. (2002) EGF receptor downregulation depends on a trafficking motif in the distal tyrosine kinase domain. *Am. J. Physiol. Cell Physiol. 282*, C420–C433.

(37) Hori, Y., Ueno, H., Mizukami, S., and Kikuchi, K. (2009) Photoactive yellow protein-based protein labeling system with turn-on fluorescence intensity. *J. Am. Chem. Soc. 131*, 16610–16611.

(38) Gendreizig, S., Kindermann, M., and Johnsson, K. (2003) Induced protein dimerization *in vivo* through covalent labeling. *J. Am. Chem. Soc. 125*, 14970–14971.

(39) Chidley, C., Mosiewicz, K., and Johnsson, K. (2008) A designed protein for the specific and covalent heteroconjugation of biomolecules. *Bioconjugate Chem. 19*, 1753–1756.

BC100333K